International Institute for Applied Systems Analysis
IIASA

Address: IIASA, Schlossplatz 1, A-2361 Laxenburg, Austria

Email: permissions@iiasa.ac.at

Working paper

A Reduced-Complexity Model of Process-Based IAMs

Johannes Bednar (bednar@iiasa.ac.at)
Artem Baklanov (baklanov@iiasa.ac.at)

WP-25-001

Approved by:

Elena Rovenskaya
Program: Advancing Systems Analysis (ASA) Program
Date: 24 August 2025

Table of contents

ZVR 524808900

The authors gratefully acknowledge funding from IIASA and the Member Organizations that support the institute. Furthermore, the authors gratefully acknowledge funding from the Grantham Foundation for the research project ‘The option value of solar radiation management in climate risk management’. Moreover, the authors gratefully acknowledge funding from the Jubiläumsfonds of the Austrian National Bank (OeNB) for the research project ’FINCRO’.

Abstract

This working document presents the development and calibration of abatement cost functions for a reduced-complexity integrated assessment model (IAM). A total of ten cost functions, partially linked to one another, are developed and calibrated based on complex process-based IAMs. This design allows the reduced-complexity model to replicate scenarios produced by more detailed IAMs while running significantly faster. The improved computational efficiency enables the exploration scenarios based on multiple parameter sets, each representing a complex IAM, to provide a robust representation of technological uncertainty.

The final model is versatile, functioning either as an optimization tool (e.g., for cost minimization under a temperature target or welfare maximization when linked to a Ramsey growth model like DICE) or as a simulation tool that takes a carbon price path as input. It is important to note that this document focuses solely on the cost functions, which form the model's core, as well as some exploratory model extensions. Other components, such as climate or economic modules, can be easily linked using existing models.

About the authors

Johannes Bednar and Artem Baklanov are research scholars in the Exploratory Modeling of Human-natural Systems Research Group of the IIASA Advancing Systems Analysis Program.

1 Model description

1.1 Model variables and index sets

In this model, various variables are indexed by specific categories to represent different aspects of energy use, emissions, and costs. Below, we define each variable along with its respective index set. A summary of the model is provided in ANNEX B.

1.1.1 Primary energy W_i

Represents the quantity of primary energy. The index i belongs to the set of primary energy types $\mathcal{I} = \{\text{foss, nbr, bio, nuc, trad}\}$, where:

- W_{foss}: Primary energy from fossil fuels
- W_{nbr}: Primary energy from non-biomass renewables
- W_{bio}: Primary energy from biomass
- W_{nuc}: Primary energy from nuclear
- W_{trad}: Primary energy from traditional biomass

1.1.2 Final energy F

Represents the quantity of final energy and encompasses all end-use energy types without differentiation. Abatement in final energy is denoted by the index fe.

1.1.3 Other emitting sectors

Emitting sectors other than the energy sector include the industrial and Agriculture, Forestry, and Other Land Use (AFOLU) sectors, which are represented by the set $\mathcal{N} = \{\text{ind}, \text{afolu}\}$.

1.1.4 Emissions E_j

Represents emissions associated with different sectors. The index j belongs to the set $\mathcal{J} = \mathcal{N} \cup \{\text{ener}\}$, where:

- E_{ener}: Pre-capture emissions from the energy system (i.e., emissions are aggregated as if no carbon capture were present)
- E_{ind}: Pre-capture industrial process emissions (e.g., cement, steel)
- E_{afolu}: Net emissions from AFOLU

1.1.5 Carbon capture S_k

Represents the amount of emissions captured and stored from the atmosphere and point sources, like fossil carbon capture and storage (CCS). The index k is associated with different capture and storage options, defined by the set $\mathcal{K} = \{\text{s\_foss, s\_bio, s\_ind, s\_dac}\}$, where:

- $S_{\text{s\_foss}}$: Carbon capture via fossil CCS
- $S_{\text{s\_bio}}$: Removals via bioenergy with CCS (BECCS)
- $S_{\text{s\_ind}}$: Carbon capture via industry CCS
- $S_{\text{s\_dac}}$: Removals via direct air CCS (DACCS)

1.1.6 Absolute abatement A_m

Represents reductions in emissions or increase of carbon capture compared to a baseline (but not expressed as fraction of baseline emissions). The index m belongs to the expanded set $\mathcal{M} = \mathcal{I} \cup \mathcal{N} \cup \mathcal{K} \cup \{\text{fe}\}$, where we have abatement through: emission reductions from primary energy substitution, industry and AFOLU emission reductions, carbon capture, as well as emission reductions from reducing final energy demand.

1.1.7 Marginal costs P_m and total costs C_m

Represent the marginal and total cost associated with each type of emission reduction or carbon capture, respectively. The index m is the same as for A_m and uses the set $\mathcal{M}$.

1.2 Model parameters

1.2.1 Carbon intensity of fossil fuels β_{foss}

We define β_{foss} as the carbon intensity of fossil fuels. A simplifying assumption is made that β_{foss} is constant, although in reality it varies depending on the fossil fuel mix. This mix may differ especially between baseline and mitigation scenarios.

1.2.2 Conversion efficiencies η_i

Conversion efficiencies η_i, where $0 < \eta_i < 1$, represent the efficiency with which primary energy is converted into final energy. These parameters capture technological and systemic losses during the conversion process (e.g., electricity generation or refining). We assume these efficiencies remain constant, even as energy end-use patterns change. The index i is defined as in Section 1.1.1.

1.2.3 Fossil fuel substitution efficiencies σ_i

The fossil fuel substitution efficiency σ_i is defined as the ratio of the conversion efficiency of energy type i to that of fossil fuels:

$$\sigma_i := \frac{\eta_i}{\eta_{\text{foss}}}$$

This parameter allows comparisons of how efficiently alternative energy sources substitute for fossil fuels in delivering final energy.

1.3 Basic model structure

Net carbon emissions from the energy, industry, and AFOLU sectors are calculated as follows:

$$E_{\text{net}}(t) = \sum_{j \in \{\text{ener,ind,afolu}\}} E_j(t) - \sum_{k \in \{\text{s\_foss,s\_bio,s\_ind,s\_dac}\}} S_k(t),$$

where $E_{\text{net}}(t)$ represents net emissions, and $E_j(t)$ denotes emissions from different sectors (see Section 1.1.4). The term $S_k(t)$ represents carbon capture from point sources or the atmosphere, as introduced in Section 1.1.5.

Pre-capture emissions from the energy sector, $E_{\text{ener}}(t)$, are calculated based on the primary fossil energy consumption $W_{\text{foss}}(t)$ and the carbon intensity of fossil fuels, β_{foss} (see Section 1.2.1):

$$E_{\text{ener}}(t) = \beta_{\text{foss}} W_{\text{foss}}(t).$$

Final energy $F(t)$ is defined as a linear function of the primary energy sources, weighted by their respective conversion efficiencies η_i, as defined in Section 1.2.2

$$F(t) = \sum_{i \in \{\text{foss,nuc,bio,trad,nbr}\}} \eta_i W_i(t).$$

From this relationship, the primary fossil energy consumption $W_{\text{foss}}(t)$ can be expressed as:

$$W_{\text{foss}}(t) = \frac{1}{\eta_{\text{foss}}} \left(F(t) - \sum_{i \in \{\text{nuc,bio,trad,nbr}\}} \eta_i W_i(t) \right). \tag{1}$$

1.4 Baseline and mitigation scenarios

To distinguish between elements from the baseline and mitigation scenarios, we introduce a hat notation. For instance, $\hat{W}_{\text{foss}}(t)$ represents the fossil primary energy in the baseline scenario. Initially, model variables are fixed to their baseline values, such that:

$$W_i(t_0) := \hat{W}_i(t_0) \quad \text{and} \quad F(t_0) := \hat{F}(t_0).$$

The same applies to carbon capture, so that:

$$S_k(t_0) := \hat{S}_k(t_0).$$

For internal consistency, the initial value of fossil primary energy, $W_{\text{foss}}(t_0)$, is calculated using Eq. (1).

1.5 Energy sector abatement

It is assumed that abatement can occur through reducing final energy $F(t)$, for example through increased efficiency or reduced demand, compared to a baseline; or by increasing other sources of zero-carbon primary energy $W_i(t)$, where $i \in \{\text{nuc}, \text{bio}, \text{nbr}\}$, compared to a baseline, thus substituting $W_{\text{foss}}(t)$. In this section, cost functions for reducing $F(t)$ and increasing $W_i(t)$ are introduced. Traditional biomass, $W_{\text{trad}}(t)$, does not represent a valid substitute for fossil fuels. It is phased-out in virtually all mitigation scenarios, with minor differences between individual scenario pathways. Moreover, the impact of carbon pricing on $W_{\text{trad}}(t)$ is not obvious, hence, it is assumed that $W_{\text{trad}}(t) := \hat{W}_{\text{trad}}(t)$.

We define abatement, $A(t)$, compared to the baseline scenario as:

$$A(t) := \beta_{\text{foss}} \left(\hat{W}_{\text{foss}}(t) - W_{\text{foss}}(t) \right). \tag{2}$$

We define $\Delta W_i(t) := \hat{W}_i(t) - W_i(t)$ and $\Delta F(t) := \hat{F}(t) - F(t)$. Because $W_{\text{trad}}(t) := \hat{W}_{\text{trad}}(t)$, $\Delta W_{\text{trad}}(t) = 0$. From (1), it follows that:

$$\Delta W_{\text{foss}}(t) = \frac{\Delta F(t)}{\eta_{\text{foss}}} - \frac{\sum_{i \in \{\text{nuc,bio,nbr}\}} \eta_i \Delta W_i(t)}{\eta_{\text{foss}}}.$$

Furthermore, combining with 2,

$$A(t) = \beta_{\text{foss}} \left(\frac{\Delta F(t)}{\eta_{\text{foss}}} - \frac{\sum_{i \in \{\text{nuc,bio,nbr}\}} \eta_i \Delta W_i(t)}{\eta_{\text{foss}}} \right).$$

Using fossil fuel substitution efficiencies $\sigma_i := \frac{\eta_i}{\eta_{\text{foss}}}$ (see Section 1.2.3), abatement can be attributed to different sources:

$$A_{\text{fe}}(t) := \frac{\beta_{\text{foss}} \Delta F(t)}{\eta_{\text{foss}}},$$

$$A_i(t) := -\beta_{\text{foss}} \sigma_i \Delta W_i(t), \quad i \in \{\text{nuc}, \text{bio}, \text{nbr}\}. \tag{3}$$

1.5.1 Cost functions for primary energy substitution

In an optimization setting, the model's objective function typically incorporates the total cost function – either directly, in the case of cost minimization, or indirectly through a utility function in an economic growth framework (e.g., welfare maximization in the DICE model). Here, we introduce such cost functions. Roughly speaking, we explain how a feasible path of $W_i(\cdot)$ (equivalently, $A_i(\cdot)$) produces paths of marginal costs $P_i(\cdot)$, and total costs $C_i(\cdot)$. In contrast, in ANNEX C we show how based on a carbon price path, $P(\cdot)$ we can compute $A_i(\cdot)$, $P_i(\cdot)$ and $C_i(\cdot)$, a process used for the calibration of the model, and running the model in a simulation setting, rather than optimization.

Marginal abatement costs, $P_i(t)$, that capture the complex process of substituting fossil fuels with alternative primary energy sources are defined as (recall that $\Delta W_i < 0$):

$$P_i(t) = \begin{cases} a_i(-\Delta W_i(t) + l_i \Delta W_i(t-1))^{b_i} + d_i, & \text{for } \Delta W_i(t) \leq l_i \Delta W_i(t-1) \\ d_i, & \text{for } \Delta W_i(t) > l_i \Delta W_i(t-1) \end{cases}$$

Using the definition for abatement, $A_i(t) = -\beta_{\text{foss}}\sigma_i \Delta W_i(t)$, we obtain:

$$P_i(t) = \begin{cases} \frac{a_i}{(\beta_{\text{foss}}\sigma_i)^{b_i}}(A_i(t) - l_i A_i(t-1))^{b_i} + d_i, & \text{for } A_i(t) \geq l_i A_i(t-1) \\ d_i, & \text{for } A_i(t) < l_i A_i(t-1) \end{cases} \tag{4}$$

The logic of the marginal cost function is as follows: Marginal costs remain constant at the floor level d_i when $A_i(t) < l_i A_i(t-1)$, but follow a power law when $A_i(t) \geq l_i A_i(t-1)$. The point at which marginal costs begin to follow a power law depends on previous abatement and the size of the lag parameter, l_i, where $0 \leq l_i \leq 1$, i.e., it is path-dependent. Larger abatement in the beginning leads to future cost functions capable of achieving greater abatement at lower average costs.

Moreover, in an optimization context, the following constraints are imposed:

$$W_i(t) \leq v_i(t), \tag{5}$$

$$A_i(t) \leq \beta_{\text{foss}}\sigma_i g_i + l_i A_i(t-1), \tag{6}$$

where $v_i(t)$ is the maximum amount of $W_i(t)$, as discussed in Section 2.5; and g_i is a growth parameter further detailed in ANNEX C. Hence, primary energy $W_i(t)$ cannot exceed $v_i(t)$; and g_i and l_i together control the maximum growth of abatement by period.

To obtain total costs from the marginal cost function for the standard case, where $A_i(t) \geq l_i A_i(t-1)$, we integrate over abatement from 0 to $A_i(t)$. Note that from Eq. 2, it follows that $A_{i,\text{min}}(t) = 0$ for $A_i(t) < l_i A_i(t-1)$, and $A_{i,\text{min}}(t) = l_i A_i(t-1)$ otherwise:

$$\begin{aligned} C_i(t) &= \int_{A_{i,\text{min}}(t)}^{A_i(t)} \left(\frac{a_i}{(\beta_{\text{foss}}\sigma_i)^{b_i}}(\widetilde{A}_i(t) - l_i A_i(t-1))^{b_i} + d_i \right) d\widetilde{A}_i \\ &= \int_{l_i A_i(t-1)}^{A_i(t)} \frac{a_i}{(\beta_{\text{foss}}\sigma_i)^{b_i}}(\widetilde{A}_i(t) - l_i A_i(t-1))^{b_i} d\widetilde{A}_i + \int_0^{A_i(t)} d_i \, d\widetilde{A}_i. \end{aligned}$$

Hence, total costs for abatement from substituting fossil fuels are:

$$C_i(t) = \begin{cases} \frac{a_i}{b_i+1}\left(\frac{1}{(\beta_{\text{foss}}\sigma_i)^{b_i}}(A_i(t) - l_i A_i(t-1))^{b_i+1} \right) + d_i A_i(t), & \text{for } A_i(t) \geq l_i A_i(t-1) \\ d_i A_i(t), & \text{for } A_i(t) < l_i A_i(t-1). \end{cases}$$

Structurally, the cost functions derived for other types of abatement are almost identical with the ones introduced here.

1.5.2 Cost functions for final energy reduction

For final energy, the objective is to decrease energy use, as opposed to increasing a substitute for fossil fuels in the case of primary energy. Hence, the cost function differs from those for primary energy substitution in terms of the signs. Marginal costs for reducing final energy are defined as:

$$P_{\text{fe}}(t) = \begin{cases} a_{\text{fe}} \left(\frac{\eta_{\text{foss}}}{\beta_{\text{foss}}}\right)^{b_{\text{fe}}} (A_{\text{fe}}(t) - l_{\text{fe}} A_{\text{fe}}(t-1))^{b_{\text{fe}}} + d_{\text{fe}}, & \text{for } A_{\text{fe}}(t) \geq l_{\text{fe}} A_{\text{fe}}(t-1) \\ d_{\text{fe}}, & \text{for } A_{\text{fe}}(t) < l_{\text{fe}} A_{\text{fe}}(t-1) \end{cases} \tag{7}$$

Moreover, in an optimization context, the following constraints are imposed:

$$F(t) \geq v_{\text{fe}}(t),$$

$$A_{\text{fe}}(t) \leq \frac{\beta_{\text{foss}}}{\eta_{\text{foss}}} g_{\text{fe}} + l_{\text{fe}} A_{\text{fe}}(t-1).$$

Here, $v_{\text{fe}}(t)$ is the minimum allowable amount of $F_i(t)$, as discussed in Section 2.5; and g_{fe} is a growth parameter, further explained in ANNEX C. As for primary energy substitution, to obtain total costs from the marginal cost function, we integrate over abatement:

$$C_{\text{fe}}(t) = \int_{A_{\text{fe, min}}(t)}^{A_{\text{fe}}(t)} \left(a_{\text{fe}} \left(\frac{\eta_{\text{foss}}}{\beta_{\text{foss}}}\right)^{b_{\text{fe}}} (\widetilde{A}_{\text{fe}}(t) - l_{\text{fe}} A_{\text{fe}}(t-1))^{b_{\text{fe}}} + d_{\text{fe}} \right) d\widetilde{A}_{\text{fe}}.$$

Hence, the total costs are:

$$C_{\text{fe}}(t) = \begin{cases} \frac{a_{\text{fe}}}{b_{\text{fe}}+1} \left(\frac{\eta_{\text{foss}}}{\beta_{\text{foss}}}\right)^{b_{\text{fe}}} (A_{\text{fe}}(t) - l_{\text{fe}} A_{\text{fe}}(t-1))^{b_{\text{fe}}+1} + d_{\text{fe}} A_{\text{fe}}(t), & \text{for } A_{\text{fe}}(t) \geq l_{\text{fe}} A_{\text{fe}}(t-1) \\ d_{\text{fe}} A_{\text{fe}}(t), & \text{for } A_{\text{fe}}(t) < l_{\text{fe}} A_{\text{fe}}(t-1). \end{cases}$$

1.6 Industry and AFOLU sector abatement

Emissions from the industry and AFOLU sectors, as in Section 1.1.4, are denoted by $E_j(t)$, where $j \in \mathcal{N} = \{\text{ind}, \text{afolu}\}$. Abatement with respect to a baseline is given as $A_j(t) := \hat{E}_j(t) - E_j(t)$. We define marginal abatement costs in these sectors as:

$$P_j(t) = \begin{cases} a_j (A_j(t) - l_j A_j(t-1))^{b_j} + d_j, & \text{for } A_j(t) \geq l_j A_j(t-1) \\ d_j, & \text{for } A_j(t) < l_j A_j(t-1). \end{cases} \tag{8}$$

and impose the following constraints for optimization:

$$A_j(t) \leq v_j(t),$$

$$A_j(t) \leq g_j + l_j A_j(t-1).$$

Here, v_j represents the maximum allowable abatement in the industry and AFOLU sectors, further detailed in Section 2.5; and g_j is a growth parameter discussed in ANNEX C. As before, a total cost function can be derived by integrating over abatement:

$$C_j(t) = \begin{cases} \frac{a_j}{b_j+1} (A_j(t) - l_j A_j(t-1))^{b_j+1} + d_j A_j(t), & \text{for } A_j(t) \geq l_j A_j(t-1) \\ d_j A_j(t), & \text{for } A_j(t) < l_j A_j(t-1). \end{cases}$$

1.7 Carbon capture

Carbon capture, denoted by $S_k(t)$ as introduced in Section 1.1.5, leads to abatement with respect to a baseline, represented by $A_k(t) := S_k(t) - \hat{S}_k(t)$. Because captured CO_2 cannot exceed the CO_2 produced during fossil fuel combustion, biofuel use, or industrial processes, we cap the amount of $S_k(t)$ for $k \in \{\text{s\_foss, s\_bio, s\_ind}\}$ as follows:

$$
\begin{aligned}
v_{\text{s\_foss}}(t) &= f^{\text{pot}}_{\text{s\_foss}}(E_{\text{ener}}(t)),\\
v_{\text{s\_bio}}(t) &= f^{\text{pot}}_{\text{s\_bio}}(W_{\text{bio}}(t)),\\
v_{\text{s\_ind}}(t) &= f^{\text{pot}}_{\text{s\_ind}}(E_{\text{ind}}(t)).
\end{aligned}
$$

The functions f_k^{pot} are explained in Section 2.4. Marginal costs of abatement through carbon capture are defined as:

$$
P_k(t) = \begin{cases} a_k \left(A_k(t) - l_k A_k(t-1)\right)^{b_k} + d_k, & \text{for } A_k(t) \geq l_k A_k(t-1) \\ d_k A_k(t), & \text{for } A_k(t) < l_k A_k(t-1). \end{cases} \tag{9}
$$

Moreover, we impose the following constraints:

$$
\begin{aligned}
S_k(t) &\leq v_k(t),\\
A_k(t) &\leq g_k + l_k A_k(t-1).
\end{aligned}
$$

The maximum allowable carbon capture quantities, v_k, for $k \in \{\text{s\_foss, s\_bio, s\_ind, s\_dac}\}$ are discussed in further detail in Section 2.5. The growth parameter, g_k, is discussed in ANNEX C. Following the same procedure as for primary energy substitution, total costs are computed by integrating over abatement. The total cost expression becomes:

$$
C_k(t) = \int_{A_{k,\text{min}}(t)}^{A_k(t)} \Big(a \left(A_k(t) - l_k A_k(t-1)\right)^{b_k} + d_k\Big)\, dA_k,
$$

which can be further broken down as:

$$
C_k(t) = \int_{l_k A_k(t-1)}^{A_k(t)} a \left(A_k - l_k A_k(t-1)\right)^{b_k} dA_k + \int_0^{A_k(t)} d_k \, dA_k.
$$

The integration yields:

$$
C_k(t) = \begin{cases} \frac{a_k}{b_k+1}(A_k(t) - l_k A_k(t-1))^{b_k+1} + d_k A_k(t), & \text{for } A_k(t) \geq l_k A_k(t-1) \\ d_k A_k(t), & \text{for } A_k(t) < l_k A_k(t-1). \end{cases}
$$

1.8 Linking carbon price with marginal costs

A general assumption of economic efficiency is expressed as:

$$
P_m(t) = P(t) \quad \forall m,
$$

meaning that the marginal abatement cost $P_m(t)$ is equal across all abatement options m. This reflects the calibration of the model to a unified carbon price, and it is recommended that this condition be upheld if the proposed cost functions are used in an optimization or simulation setting. However, due to the various constraints imposed on abatement, such as Eqs. 5 and 6, there are implied marginal cost caps and floors which vary between abatement options. Therefore, the condition, $P_m(t) = P(t) \quad \forall m$, is generally not met by the marginal cost functions introduced in Sections 1.5 through 1.7. In ANNEX C, and more specifically in C.1.1 we illustrate how marginal costs can be kept consistent with a unified carbon price P.

2 Model calibration

- **Data source**: We use data from the ENGAGE model intercomparison, available in the AR6 database. The scenarios are based on the socioeconomic pathway of SSP2.
- **Data structure**: The dataset is organized by model, scenario, and year. Different near-term policy assumptions, as well as overshoot and non-overshoot scenarios for the same carbon budget, are present. However, for calibration purposes, these distinctions are not considered.
- **Parameter sets**: A parameter set is calibrated for each complex IAM included in the dataset.
- **Component Calibration**: Each component, such as cost functions, is calibrated individually rather than optimizing parameters for the entire model simultaneously.
- **Notation**: Throughout this document, lowercase letters refer to variables from the dataset, while uppercase letters denote modeled variables used in the equations.
- **Abatement notation**: To prevent confusion with the cost function coefficients, abatement from the dataset is denoted by $x_m(t)$, defined as:

  $$x_m(t) = \hat{e}_m(t) - e_m(t),$$

  where $\hat{e}_m(t)$ and $e_m(t)$ represent baseline and mitigation scenario emissions from the dataset, respectively.

2.1 Data preparation and polishing

The following steps are applied prior to calibration to ensure consistent and meaningful data:

- **Scenario filtering**: We exclude
  - COVID-related scenarios, identified by "COV" in the scenario name,
  - Sensitivity analysis scenarios, identified by "NDCp",
  - Scenarios with non-standard discount rates, identified by "DR",
  - All scenarios from the COFFEE 1.1 and POLES ENGAGE IAMs due to data gaps and inconsistencies that could not be reliably corrected.
- **IAM-specific adjustments**:
  - For **GEM-E3_V2021**, `Carbon Sequestration|CCS|Biomass` is missing from the AR6 database. We instead retrieve `Primary Energy|Biomass|Modern|w/ CCS` from the ENGAGE-native database and infer biomass sequestration using assumed capture efficiencies.
  - For **IMAGE 3.0** AFOLU emissions increase in mitigation scenarios compared to the baseline, which is incompatible with the defined cost functions. AFOLU emissions are therefore set to an average path of mitigation scenarios. Costs are assumed to be zero. The scenario `EN_INDCi2030_1400f` is removed because the reported carbon price is 0.

  - For **WITCH 5.0**, we observe inconsistencies in CO2 emissions in relation to fossil energy consumption. To correct this:
    * We add `Emissions|CO2|Industrial Processes` to `Emissions|CO2|Energy` and set industrial emissions to zero.
    * This adjustment ensures that pre-capture emissions (i.e., energy emissions plus captured emissions) remain non-negative in regional data and consistent with primary fossil energy use.
  - We harmonize `Primary Energy|Biomass|Traditional` across scenarios by replacing scenario-specific trajectories with the median trajectory for each IAM across all scenarios. Traditional biomass is phased-out in all scenarios.

- **DACCS Energy Correction**: DACCS is only available in scenarios from the models WITCH 5.0 and REMIND-MAGPIE 2.1-4.2. The reported final and primary energy uses includes the energy consumed by DACCS. To avoid overestimating the energy actually used for economic activities, we correct final and primary energy by removing the share attributable to DACCS.

  DACCS energy demand per tonne of CO_2 is assumed to be 6.9 GJ heat and 1.55 GJ electricity in WITCH 5.0, and 10 GJ heat and 2 GJ electricity in REMIND-MAGPIE 2.1-4.2, based on literature (Realmonte et al. [2019]) and model documentation (PIK Potsdam Institute for Climate Impact Research). From scenario data we infer that the energy carriers used to supply this demand differ: in WITCH 5.0, heat is assumed to be primarily provided by natural gas (80%, vs. 20% from hydrogen), whereas in REMIND-MAGPIE 2.1-4.2, it comes almost entirely from hydrogen (95%, vs. 5% from natural gas), which is itself produced from electricity and fossil fuels. Electricity for DACCS, including electricity used indirectly for hydrogen production, is assumed to come fully from NBRs in both IAMs, which is consistent with the high renewable shares observed in their DACCS-intensive scenarios.

  The source shares for hydrogen (electricity vs. fossil) and the efficiencies of various conversion processes are either assumed or inferred directly from the scenario data. This allows us to attribute DACCS energy demand back to primary energy carriers.

  We then correct both final energy (by subtracting the total DACCS energy demand) and primary energy (by subtracting the upstream energy used to supply DACCS heat and electricity). For WITCH 5.0, an additional correction is made to the accounting of fossil fuels with and without CCS, since gas used for DACCS appears to be reported inconsistently across those categories. We resolve this by reallocating gas energy and adjusting reported fossil CCS capture accordingly.

2.2 Carbon intensity

For the calibration of the carbon intensity of fossil fuels β_{foss}, we use a simple linear regression model of the form:

$$e_{\text{ener}}(t) \sim \beta_{\text{foss}} w_{\text{foss}}(t)$$

where $e_{\text{ener}}(t)$ denotes pre-capture emissions from the energy sector, and $w_{\text{foss}}(t)$ represents primary energy consumption from fossil fuels. The results for each IAM are summarized in Table 1.

Model	β_{foss}
AIM/CGE 2.2	68
GEM-E3_V2021	61
IMAGE 3.0	69
MESSAGEix-GLOBIOM_1.1	70
TIAM-ECN 1.1	65
REMIND-MAgPIE 2.1-4.2	70
WITCH 5.0	67

Table 1: Estimated carbon intensity of fossil fuels (β_{foss}) in MtCO2/EJ for various IAMs

2.3 Energy conversion

We estimate the energy conversion efficiencies between primary energy, $w_i(t)$, and final energy, $f(t)$, with a linear regression model of the form:

$$f(t) \sim \sum_{i \in \{\text{foss,nuc,bio,trad,nbr}\}} \eta_i w_i(t).$$

However, estimating these conversion efficiencies individually for each IAM is challenging due to the high degree of multicollinearity between the primary energy sources. To overcome this, we employ a two-stage calibration approach:

2.3.1 Initial calibration using data from all IAMs

In the first stage, we combine data from all IAMs. This significantly reduces collinearity among the primary energy sources, with variance inflation factors (VIF) values below 5, indicating moderate but acceptable multicollinearity.

In this stage, we use a Bayesian linear regression approach to estimate the coefficients η_i for each primary energy source, w_i.

We assign uninformative priors (uniform distribution between 0 and 1) to most coefficients. The exception is nuclear energy, where we impose a prior between 0.7 and 0.9 due to its significantly smaller scale in scenarios compared to other energy sources, making the estimate unreliable. Moreover, for traditional biomass, w_{trad}, we follow the convention that primary and final energy are the same, fixing the parameter η_{trad} to 1 through the prior.

2.3.2 IAM-specific calibration using informative priors

In the second stage, we perform the calibration for each IAM separately. To address multicollinearity issues that arise when fitting the model to individual IAM data, we use informative priors based on the results from the first stage. The expected values (means) of the coefficients η_i from the initial calibration are used as the means of normal distributions as priors, with a narrow standard deviation of 0.01. This ensures that the estimates for each IAM remain consistent with the global calibration while allowing for model-specific variation. We keep the prior for nuclear energy uniform between 0.7 and 0.9.

Model	η_{bio}	η_{nbr}	η_{nuc}	η_{foss}
AIM/CGE 2.2	0.53 ± 0.01	0.78 ± 0.01	0.82 ± 0.05	0.68 ± 0
GEM-E3_V2021	0.56 ± 0.01	0.81 ± 0.01	0.79 ± 0.06	0.75 ± 0
IMAGE 3.0	0.53 ± 0.01	0.80 ± 0.01	0.74 ± 0.03	0.73 ± 0
MESSAGEix-GLOBIOM_1.1	0.52 ± 0.01	0.88 ± 0.01	0.83 ± 0.03	0.78 ± 0
TIAM-ECN 1.1	0.53 ± 0.01	0.80 ± 0.01	0.82 ± 0.05	0.74 ± 0.01
REMIND-MAgPIE 2.1-4.2	0.53 ± 0.01	0.76 ± 0	0.83 ± 0.05	0.78 ± 0
WITCH 5.0	0.43 ± 0.01	0.79 ± 0.01	0.74 ± 0.04	0.66 ± 0

Table 2: Estimated energy conversion efficiencies (η) for various IAMs.

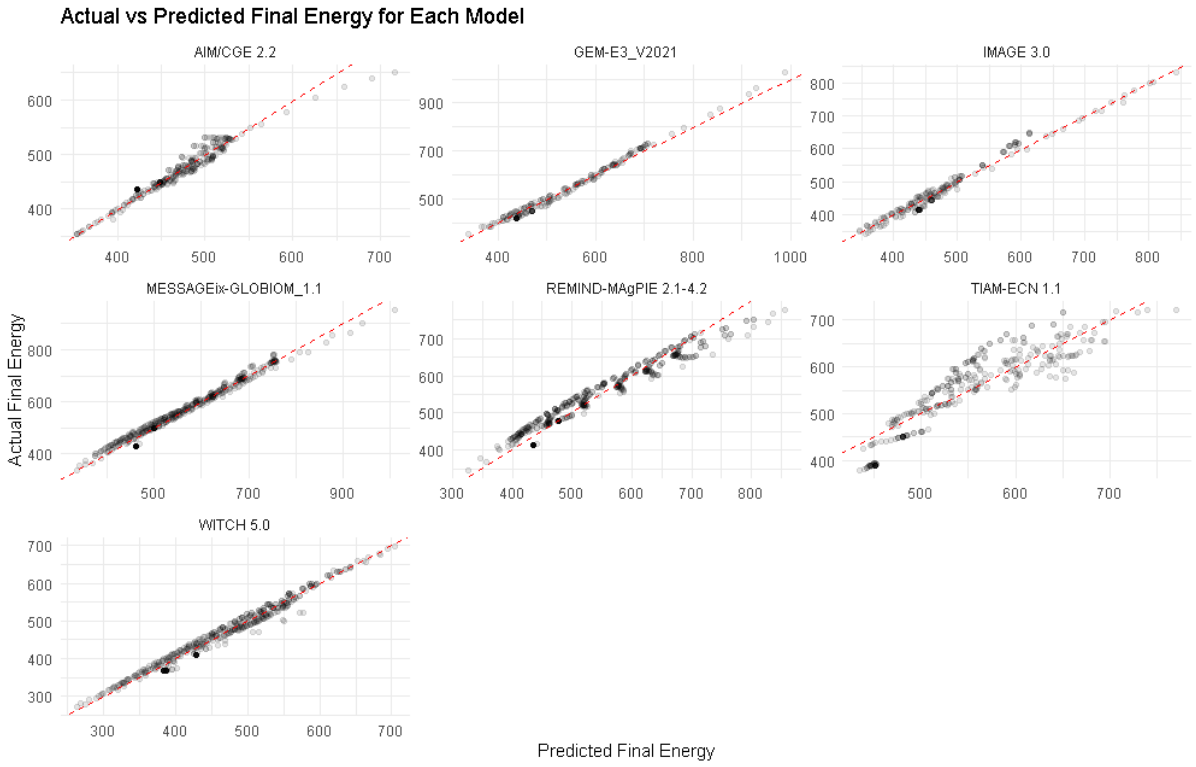

Figure 1: Actual vs. predicted final energy using energy conversion efficiencies (η) Table 2

2.3.3 Results

The energy conversion efficiencies for each IAM are shown in Table 2. Actual versus predicted final energy is shown for each IAM in Figure 1.

The fossil fuel substitution efficiencies, denoted as $\sigma_i := \frac{\eta_i}{\eta_{\text{foss}}}$, are presented in Table 3. These efficiencies measure how effectively different energy sources can substitute for fossil fuels in terms of energy conversion.

2.4 Carbon capture potentials

We compute the potentials for bioenergy CCS and industry CCS by analyzing the maximum ratio of carbon captured to the corresponding primary energy or emissions in the dataset. The maximum ratios obtained for each IAM are summarized in Table 4.

Fossil CCS is modeled differently due to several factors. Unlike bioenergy, which increases with stricter climate policies, fossil fuel use generally declines, leading to the temporary deployment of fossil CCS

Model	σ_{bio}	σ_{nbr}	σ_{nuc}
AIM/CGE 2.2	0.78 ± 0.01	1.16 ± 0.01	1.21 ± 0.08
GEM-E3$_V$2021	0.75 ± 0.01	1.09 ± 0.01	1.06 ± 0.08
IMAGE 3.0	0.72 ± 0.01	1.09 ± 0.01	1.00 ± 0.04
MESSAGEix-GLOBIOM$_1$.1	0.67 ± 0.01	1.12 ± 0.01	1.06 ± 0.04
TIAM-ECN 1.1	0.72 ± 0.01	1.08 ± 0.01	1.11 ± 0.08
REMIND-MAgPIE 2.1-4.2	0.68 ± 0.01	0.97 ± 0.01	1.06 ± 0.07
WITCH 5.0	0.65 ± 0.01	1.20 ± 0.01	1.12 ± 0.06

Table 3: Fossil fuel substitution efficiencies $\sigma_i := \frac{\eta_i}{\eta_{\text{foss}}}$ for various IAMs.

in many scenarios until fossil point sources are phased out. Additionally, bioenergy is mostly used for BECCS, creating a clear link between bioenergy consumption and carbon capture, while fossil fuel end-uses are more diverse, making it harder to directly relate fossil fuel use to CCS potential. Although similar issues might arise with industrial emissions, fossil CCS is significantly larger in scale, allowing for a simplified approach to industry CCS.

We compute CCS potentials for each IAM as follows:

2.4.1 Bioenergy CCS potential

We calculate the maximum ratio of carbon captured from bioenergy, s_{bio}, to primary bioenergy consumption, w_{bio}, over all time steps and over all scenarios for each IAM from the dataset and define bioenergy CCS potential, $v^{\text{pot}}_{\text{s\_bio}}$, as:

$$v^{\text{pot}}_{\text{s\_bio}}(t) = \max\left(\frac{s_{\text{bio}}}{w_{\text{bio}}}\right) \; W_{\text{bio}}(t)$$

Note, W_{bio} refers to the modeled value of bioenergy consumption, while w_{bio} is the dataset value of bioenergy consumption.

2.4.2 Industry CCS potential

Similarly, we compute the maximum ratio of industrial CCS, s_{ind}, to industrial process emissions, e_{ind}, from the dataset and define the industry CCS potential, $v^{\text{pot}}_{\text{s\_ind}}$, as:

$$v^{\text{pot}}_{\text{s\_ind}}(t) = \max\left(\frac{s_{\text{ind}}}{e_{\text{ind}}}\right) \; E_{\text{ind}}(t)$$

Again, E_{ind} refers to the modeled value of industrial emissions, while e_{ind} is the dataset value of industrial emissions.

2.4.3 Fossil CCS potential

In our empirical approach, the fossil CCS potential, $v^{\text{pot}}_{\text{s\_foss}}$, is modeled as an increasing piecewise linear function of pre-capture energy system emissions, e_{ener}, as exemplified in Figure 2. This function is derived from the left-side increasing portion of the convex hull over the points $(e_{\text{ener}}, s_{\text{s\_foss}})$. The function is constrained to prevent any positive intercept, ensuring that the CCS potential is zero when $e_{\text{ener}} = 0$.

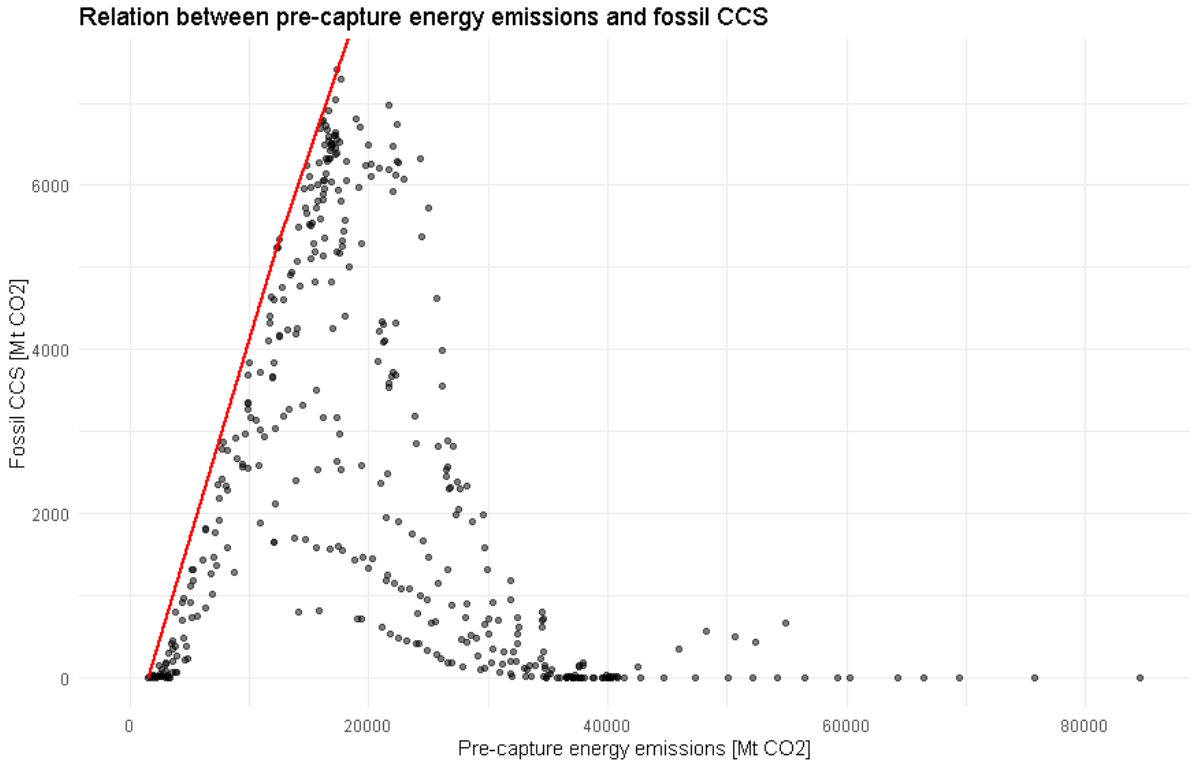

Figure 2: Red line is the fossil CCS potential for MESSAGEix-GLOBIOM 1.1

Model	$\max\left(\frac{s_{\text{bio}}}{w_{\text{bio}}}\right)$	$\max\left(\frac{s_{\text{ind}}}{e_{\text{ind}}}\right)$
AIM/CGE 2.2	63.5	0.359
GEM-E3_V2021	33.7	0
IMAGE 3.0	86.1	0.968
MESSAGEix-GLOBIOM_1.1	56.8	0.531
REMIND-MAgPIE 2.1-4.2	49.7	0.756
TIAM-ECN 1.1	66.0	0
WITCH 5.0	44.9	NA

Table 4: Maximum capture ratios for bioenergy with CCS and industry CCS from the dataset. A value of 0 indicates that there is no industry CCS in the data, while NA indicates that there are no industry emissions in the data. These ratios are used to calculate carbon capture potentials, $v^{\text{pot}}_{\text{s\_bio}}$ and $v^{\text{pot}}_{\text{s\_ind}}$, based on modeled values of W_{bio} and E_{ind}.

2.5 Variable bounds

In this section, we define the variable bounds, denoted by $v_m(t)$, which are calculated as the maximum (or minimum) reported values within each time step, across all scenarios and for each IAM of the dataset. These bounds serve to constrain the potential range of key variables, ensuring that their modeled values remain within plausible limits over time. For instance, see the variable bounds for primary bioenergy in Figure 3. Note that the bounds for carbon capture are based on the potentials outlined in the previous section, hence, they depend on model variables.

The following relationships are used to determine the bounds for each time step t:

For primary energy, the bounds at each time step are:

$$v_i(t) = \max(w_i(t)), \quad i \in \{\mathsf{nbr}, \mathsf{bio}, \mathsf{nuc}\},$$

For carbon capture, the bounds at each time step are:

$$v_k(t) = \min\left(\max(s_k(t)), v_k^{\mathsf{pot}}(t)\right), \quad k \in \{\mathsf{s\_bio}, \mathsf{s\_foss}, \mathsf{s\_ind}\},$$
$$v_{\mathsf{s\_dac}}(t) = \max(s_{\mathsf{s\_dac}}(t))$$

For abatement in the AFOLU and industry sectors, the bounds at each time step are:

$$v_{\mathsf{ind}}(t) = \max(a_{\mathsf{ind}}(t)),$$
$$v_{\mathsf{afolu}}(t) = \max(a_{\mathsf{afolu}}(t)).$$

Finally, for final energy, the bound at each time step is:

$$v_{\mathsf{fe}}(t) = \min(f(t)).$$

2.6 Model validation

2.6.1 Energy and emissions

Table 5 reports the root mean square error (RMSE) and coefficient of determination (R^2) for each parameter set (IAM), measuring the goodness of fit between modeled and reported net emissions under the reported carbon price scenarios.

Reported versus modeled values for primary energy, final energy, and emissions across all available abatement options are presented in Figures 9 through 15 in Appendix A for each parameter set (IAM) individually. The resulting net emissions pathway, derived from the combination of all model components, is also shown.

2.6.2 Average costs

Abatement costs are generally not explicitly reported for mitigation scenarios, and the calibration of cost functions in this model targets energy or emissions quantities rather than costs directly. To ensure

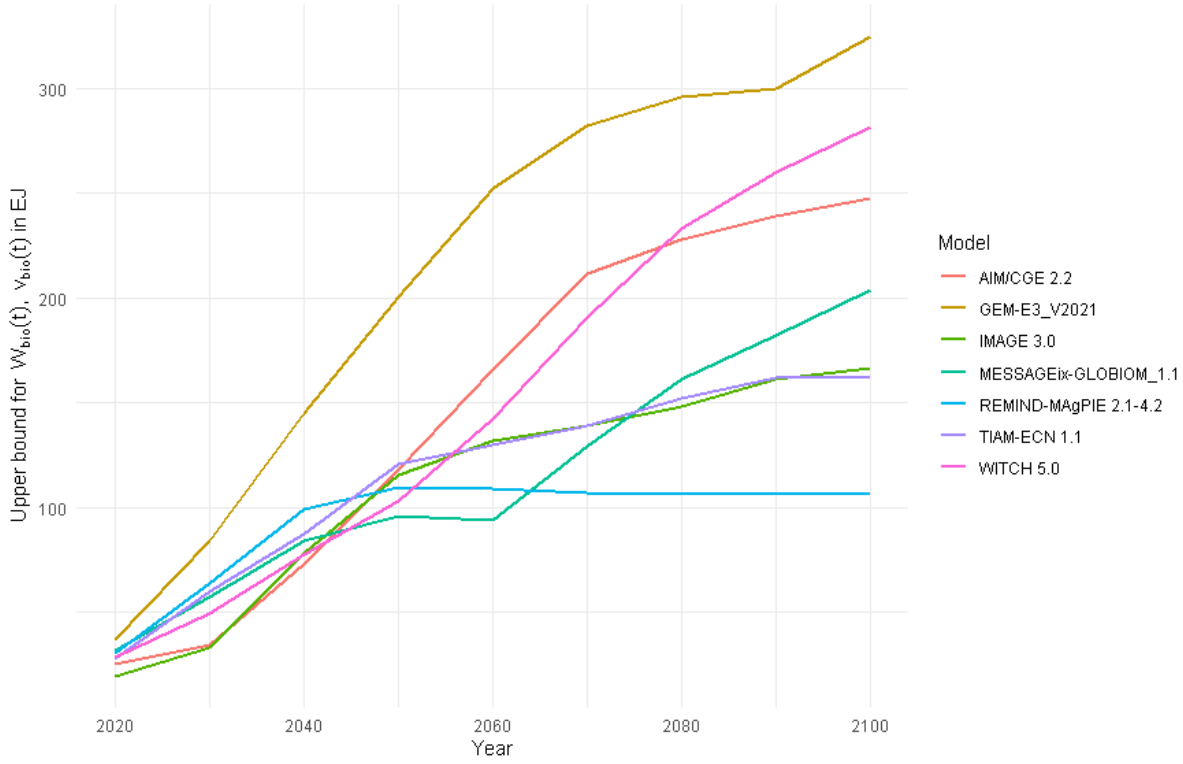

Figure 3: Upper variable bound for $W_{\text{bio}}(t)$.

Model	**RMSE [GtCO$_2$]**	R^2
AIM/CGE 2.2	2.53	0.978
GEM-E3_V2021	2.67	0.974
IMAGE 3.0	3.89	0.951
MESSAGEix-GLOBIOM_1.1	5.11	0.926
TIAM-ECN 1.1	4.49	0.935
REMIND-MAgPIE 2.1-4.2	4.77	0.914
WITCH 5.0	2.31	0.977

Table 5: Goodness-of-fit metrics from comparing all reported scenario time series with modeled pathways for each IAM. RMSE and R^2 values assess how well modeled net emissions match reported data under different carbon price scenarios, as illustrated in Figures 9 through 15.

consistency with external cost estimates, we impose soft lower bounds on the average cost of each abatement option. If the median of modeled average costs across scenarios for a given abatement option falls below its respective bound, a penalty is applied during calibration.

These bounds are median values estimated through visual interpretation of Figure SPM.7 in IPCC [2022]. However, two important limitations should be acknowledged. First, the categorization of abatement options in the IPCC figure does not align precisely with those used in our model. This mismatch is particularly evident in the treatment of final energy demand reductions, for which no meaningful bound could be derived. Second, the figure reports only cost ranges, and median values are not explicitly provided. The estimated medians, which serve as soft cost floors during calibration, are summarized in Table 6. The modeled average cost distributions are illustrated in Figure 4.

Abatement option	**Est. Median**	**Low**	**High**
Non-biomass Renewables	0	0	100
Nuclear	35	0	200
Bioenergy	80	20	200
AFOLU	50	0	200
Industry	35	0	200
CCS–Fossil	80	50	200
CCS–Bio	80	50	200
CCS–Industry	150	100	200

Table 6: Estimated median average costs in USD/tCO_2 for abatement options used in the model. A penalty is applied during calibration if the median modeled abatement cost falls below the estimated median. The lower and upper bounds represent the estimated ranges derived from IPCC AR6 WGIII Figure SPM.7.

Additionally, modeled total average abatement costs are compared against the reported consumption loss per ton of abated CO_2, where available. While consumption loss is generally considered a reasonable proxy for abatement costs, this relationship does not hold for AIM/CGE 2.2, where reported consumption loss frequently exceeds the carbon price. In simpler economic models such as DICE, this would imply that average costs exceed marginal costs, a conceptually inconsistent outcome. The discrepancy may reflect model-specific assumptions or dynamics not fully reflected here. This comparison is illustrated in Figure 16 in Appendix A.

2.7 Non-CO2 radiative forcing

We estimate non-CO_2 radiative forcing $r_{\mathrm{nonCO2}}(t)$ from fossil primary energy $w_{\mathrm{foss}}(t)$ via

$$r_{\mathrm{nonCO2}}(t) = \exp(\kappa + \gamma_1\, w_{\mathrm{foss}}(t) + \gamma_2\, w_{\mathrm{foss}}(t)^{\rho})\,.$$

Parameters are estimated per IAM and across all IAMs to inform parameter sets where no non-CO_2 radiative forcing was reported. The relationship $w_{\mathrm{foss}}(t)$ vs. $r_{\mathrm{nonCO2}}(t)$ is shown in Figure 5. Model skill is shown in Figure 6, comparing reported and predicted $r_{\mathrm{nonCO2}}(t)$.

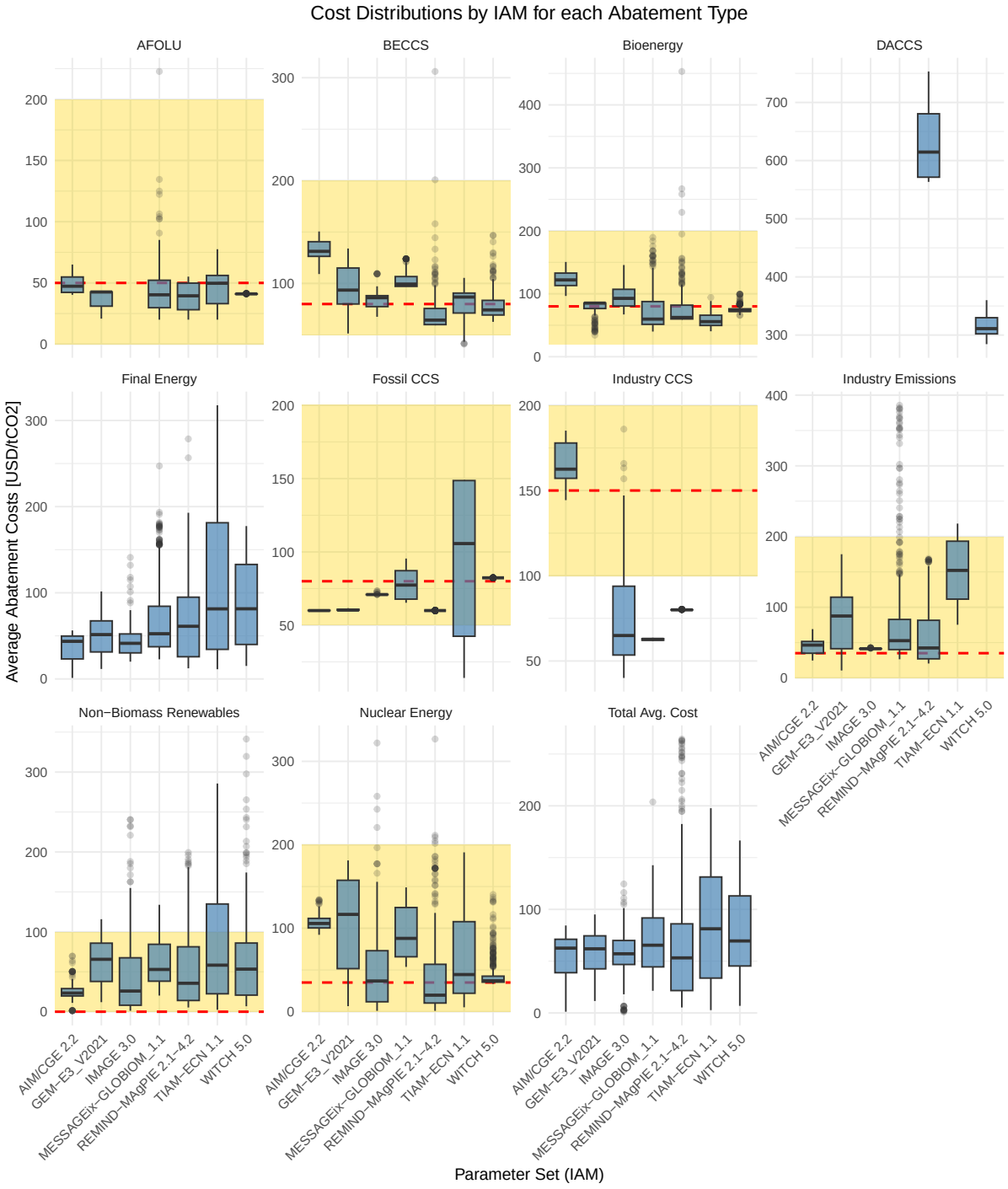

Figure 4: Distribution of average abatement costs by parameter set (IAM) across abatement types. Boxplots represent the interquartile range, median, and outliers of modeled cost estimates for each abatement option and IAM. Shaded yellow ribbons indicate the cost ranges, while the dashed line shows the soft lower cost bound as listed in Table 6. Panels are scaled individually for readability. This visualization supports the evaluation of whether models stay within plausible cost corridors for different abatement options.

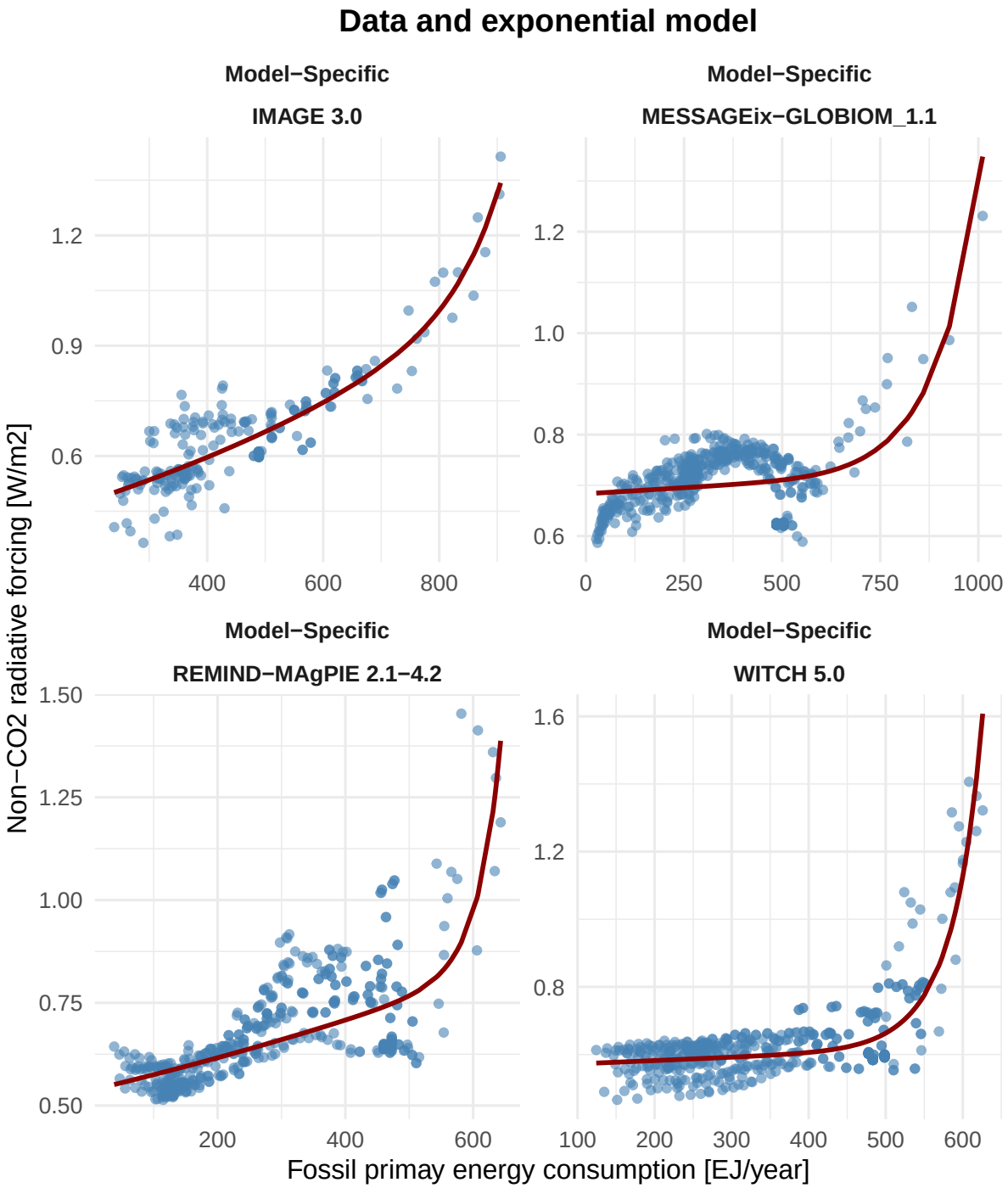

Figure 5: Relationship between fossil primary energy consumption $w_{\text{foss}}(t)$ and non-CO_2 radiative forcing $r_{\text{nonCO2}}(t)$ with fitted exponential model.

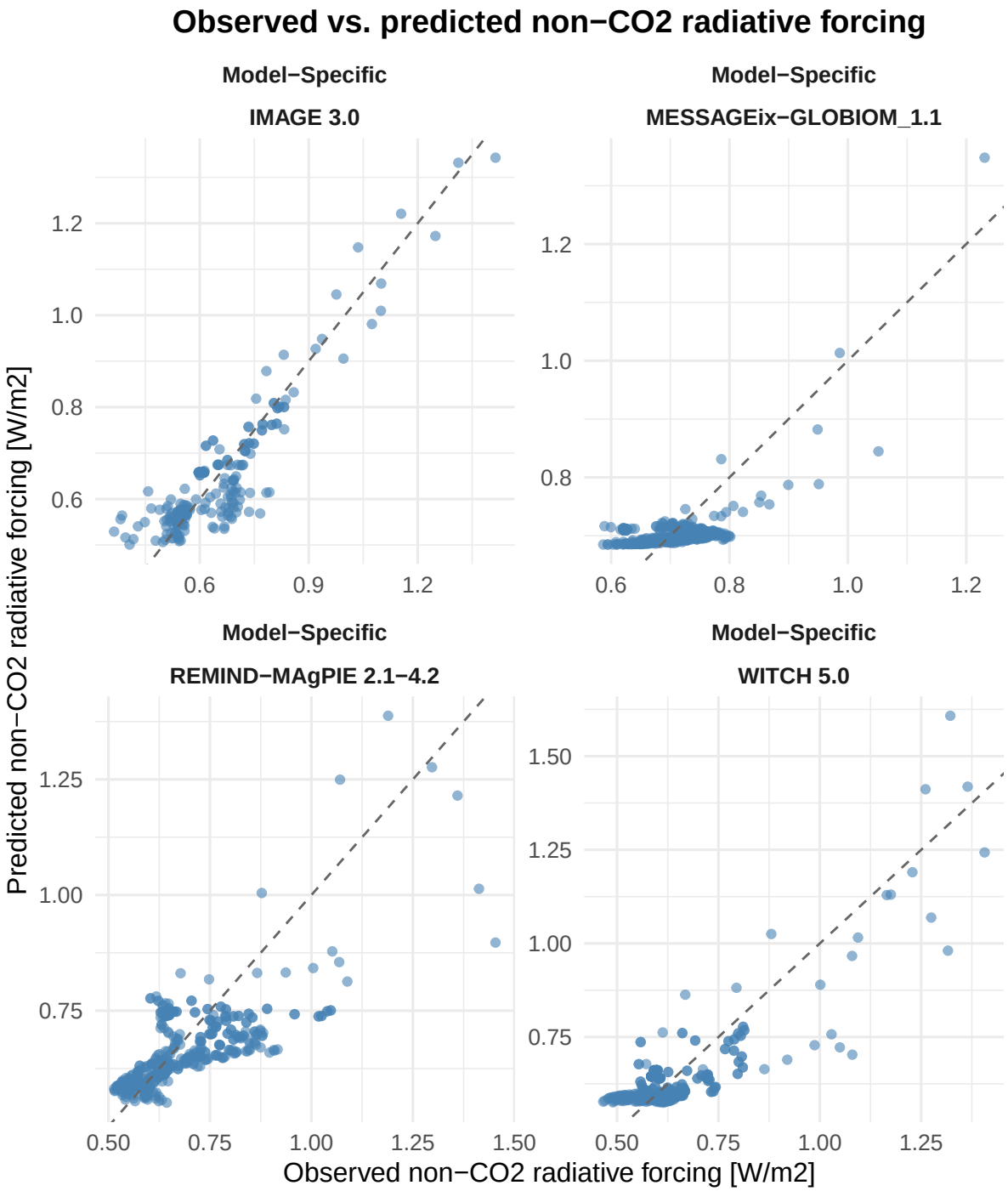

Figure 6: Observed versus predicted non-CO_2 radiative forcing $r_{\mathrm{nonCO2}}(t)$ for individual IAMs.

3 Exploratory model modifications

This section outlines a set of exploratory modifications to the calibrated model, aimed at extending its applicability beyond the scope of reported scenario data.

3.1 Integration of DACCS into all parameter sets

DACCS is incorporated as an abatement option into all model parameter sets, including those in which it was not originally reported. We use a lower-cost parameter set from WITCH 5.0 and a higher-cost parameter set from REMIND-MAgPIE 2.1-4.2 (see Figure 4). Each of these DACCS configurations is combined with the parameter set for all other abatement types from each IAM, resulting in a total of 14 model parameter sets (2 DACCS variants × 7 IAMs).

3.2 Extension of time horizon

The model's temporal scope is extended beyond 2100 to explore the long-term implications of mitigation strategies beyond the typical reporting window of IAMs. The key points of this extrapolation include:

- For consistency, the full range of abatement types is extrapolated beyond 2100. However, not all components continue to be modeled as functions of the carbon price, as they are before 2100.
- Fossil fuel emissions follow a predefined linear phase-out trajectory and are no longer price-responsive after 2100.
- Fossil fuel emissions serve as the basis for fossil CCS deployment, which continues to be determined by the carbon price, as in the pre-2100 period.
- Bioenergy and nuclear energy remain functions of the carbon price. Their deployment remains capped at the maximum levels observed between 2020 and 2100 in scenarios. Extrapolation requires an extension of baseline assumptions.
- Bioenergy serves as the basis for BECCS deployment, which continues to be determined by the carbon price.
- NBRs are assumed to meet the residual energy demand not covered by other sources, justified by their vast physical potential. NBRs are thus no functions of the carbon price post-2100.
- The baseline energy supply is extrapolated under the assumption that the fractional (i.e., relative) energy mix, such as the share of bioenergy in total primary energy, remains constant beyond 2100 at its 2100 level. This requires projecting total energy demand forward.
- Energy demand is extrapolated using a DICE-like approach in which energy demand is inferred from economic output, which itself is driven by exogenous projections of population and factor productivity growth.
- DACCS remains modeled as a function of the carbon price beyond 2100. However, the upper bound from the 2020–2100 period is imposed to reflect limits on deployment potential.

- The AFOLU sector, which typically acts as a net carbon sink before 2100 in most scenarios, is gradually phased toward net-zero emissions in the post-2100 period.
- Although long-term extrapolations inherently involve large uncertainty, several factors limit the spread between post-2100 trajectories:
  - Long-term net emissions are guided by residual fossil fuel emissions, as well as CDR.
  - Fossil fuel emissions follow a fixed phase-out path, independent of economic or policy assumptions. Bioenergy deployment, as basis for BECCS, is bounded by sustainability constraints commonly embedded in IAMs. In ambitious mitigation scenarios, these bounds are typically hit already before 2100. As a result, uncertainties in future GDP or energy demand affect only the timing at which upper limits of bioenergy are reached. Similarly, DACCS upper bounds from the 2020-2100 periods are maintained.
  - In other words, under a sufficiently high carbon price, such as one following a Hotelling-rule growth path, scenarios tend to converge toward similar long-run net-negative emissions trajectories.
- Modeled abatement costs are only credible for the period until 2100.

3.2.1 Extrapolation of population and economic output

We use a discrete-time Solow-style growth model to simulate economic output and capital accumulation with a fixed savings rate in the post-2100 period. This, in turn, is used to determine future energy demand. The model's production function, with output $Y(t)$, population $L(t)$, total factor productivity (TFP) $\alpha(t)$ and capital elasticity γ is given by:

$$Y(t) = \alpha(t)L(t)^{1-\gamma}K(t)^{\gamma}$$

Population extension for SSP2 Population trajectories are extended by blending the reported IAM-specific population projection for 2100, $L(2100)$, with an extended SSP2 population pathway, $L_{\mathrm{SSP2}}(t)$, that runs to 2300. The scaling ratio

$$r_L = \frac{L(2100)}{L_{\mathrm{SSP2}}(2100)}$$

is applied with a linearly decaying weight

$$w(t) = \frac{2300 - t}{200}$$

to yield

$$L(t) = L_{\mathrm{SSP2}}(t) \cdot r_L^{w(t)}, \quad t > 2100.$$

This approach ensures asymptotically converging to the extended SSP2 trajectory by 2300.

The L_{SSP2} pathway was obtained from IIASA's POPJUS program. The series until 2100 follows the updated SSP population scenario in K.C. et al. [2024]. For the extension to 2300, the same assumptions as to 2100 were maintained, with the exception that the fertility rate converges to 1.75 children per woman by the year 2200 for all countries, and the maximum life expectancy is set at 105 years for both sexes.

Extrapolation of economic output We first infer $\alpha(t)$ by rearranging the production function using scenario data for output and population:

$$\alpha(t) = \frac{Y(t)}{L(t)^{1-\gamma}K(t)^{\gamma}}$$

Investment is derived from reported output and consumption, $C(t)$:

$$I(t) = Y(t) - C(t)$$

Capital then evolves according to the standard discrete-time capital accumulation equation, with capital depreciation δ:

$$K(t+1) = (1 - \delta\Delta t)K(t) + \Delta t \cdot I(t)$$

We initialize capital in the first time step at 210 trillion USD (2010), based on data from the Penn World Table version 10.01 Feenstra et al. [2015].

We compute TFP $\alpha(t)$ for capital elasticity $\gamma = 0.35$, as in Leimbach et al. [2017] for SSP2, and capital depreciation $\delta = 0.1$, as in Barrage and Nordhaus [2024]. An exponential function is then fitted to the resulting TFP trajectories:

$$\alpha(t) = Ae^{bt}$$

To account for declining productivity growth post-2100, the estimated growth rate b is adjusted using an exponential decay:

$$b(t) = b \cdot e^{-\lambda(t-2100)}$$

TFP is then extrapolated recursively, following the logic of DICE 2023 (Barrage and Nordhaus [2024]), where the decline rate is set to $\lambda = 0.0075$:

$$\alpha(t) = \alpha(t-1) \cdot e^{b(t)}$$

The savings rate, defined as $s(t) = \frac{I(t)}{Y(t)}$, is assumed to converge linearly from its 2100 baseline scenario value to a fixed level of $s = 0.20$ by 2200 after which it remains constant. This reflects a moderate, 'middle-of-the-road' investment level consistent with the SSP design principle of convergence to medium capital intensities. Using the Solow growth model, the savings rate, and the extrapolated TFP trajectories, we generate a set of economic growth pathways, presented in Figure 7.

3.2.2 Abatement post 2100

For all abatement options other than NBRs, cost functions and imposed upper bounds on abatement, as introduced in Section 2.5, are assumed to remain valid beyond 2100, and their baselines are accordingly extended. NBRs are expected to grow beyond any values observed in scenarios up to 2100 and are therefore determined using a different logic (see Section 3.2.3).

Extrapolation of baselines Extrapolation of baseline scenarios is required for all abatement options other than NBRs,. We begin by extending the baseline for total primary energy. Let $\hat{W}(t)$ denote total primary energy consumption of baseline scenarios and $Y(t)$ economic output as described in

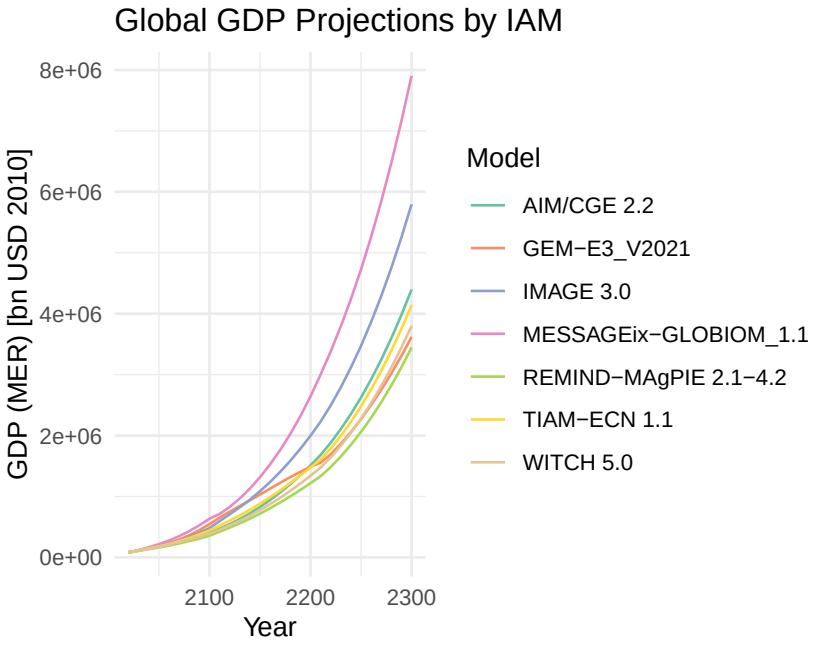

Figure 7: Extrapolated global GDP trajectories by IAM, in billion 2010 USD.

Section 3.2.1. We define the primary energy intensity

$$\phi(t) = \frac{\hat{W}(t)}{Y(t)}$$

using reported values for $\hat{W}(t)$ and $Y(t)$ over 2020–2100. We apply a hyperbolic decay function to extend primay energy intensity beyond 2100:

$$\phi(t) = \frac{\phi(2100)}{1 + \left(-\frac{\dot{\phi}(2100)}{\phi(2100)}\right) \cdot (t - 2100)},$$

where $\dot{\phi}(2100)$ denotes the derivative at $t = 2100$. Combining the extended $\phi(t)$, as illustrated for all IAMs in Figure 8, with $Y(t)$ yields the extended total primary energy path $\hat{W}(t)$ up to 2300.

Primary nuclear and bioenergy shares of $\hat{W}(t)$ are held constant at 2100 levels, implying proportional growth of $\hat{W}_{\text{bio}}$ and $\hat{W}_{\text{nuc}}$ with $\hat{W}$ after 2100 until any predefined upper bounds (see Section 2.5) are reached.

Other baselines are extended as follows: Similar to energy intensity, industrial emissions intensity is extrapolated by fitting a log-linear relationship over 2020–2100, i.e. $\log \frac{\hat{E}_{\text{ind}}(t)}{Y(t)} \sim t$. AFOLU emissions are extended by first estimating a linear trend in emissions for the period after 2050, and then applying a logistic scaling factor $(1 + \exp(0.1\,(t - 2150)))^{-1}$to that trend, such that net (negative) AFOLU emissions smoothly transition towards net zero with an inflection point at 2150. Like industry emissions intensity, traditional biomass use, W_{trad}, is extrapolated using a log-linear fit. For industry CCS, $\hat{S}_{\text{s\_ind}}$, and BECCS, $\hat{S}_{\text{s\_bio}}$, the share relative to the baseline activity, $\hat{E}_{\text{ind}}$ and $\hat{W}_{\text{bio}}$, respectively, is held constant at its 2100 value, subject to any applicable upper bounds. CCS on fossil fuels ($\hat{S}_{\text{s\_foss}}$) is phased out after 2100 with the expectation that fossil fuels are being phased out (see Section 3.2.3). Note, however, that only few baseline scenarios feature CCS, and none of them feature DACCS. Final energy is extrapolated as $\hat{F}(t) = \eta_{\text{tot}}\,\hat{W}(t)$, where η_{tot} is the total final-to-primary energy conversion efficiency in 2100.

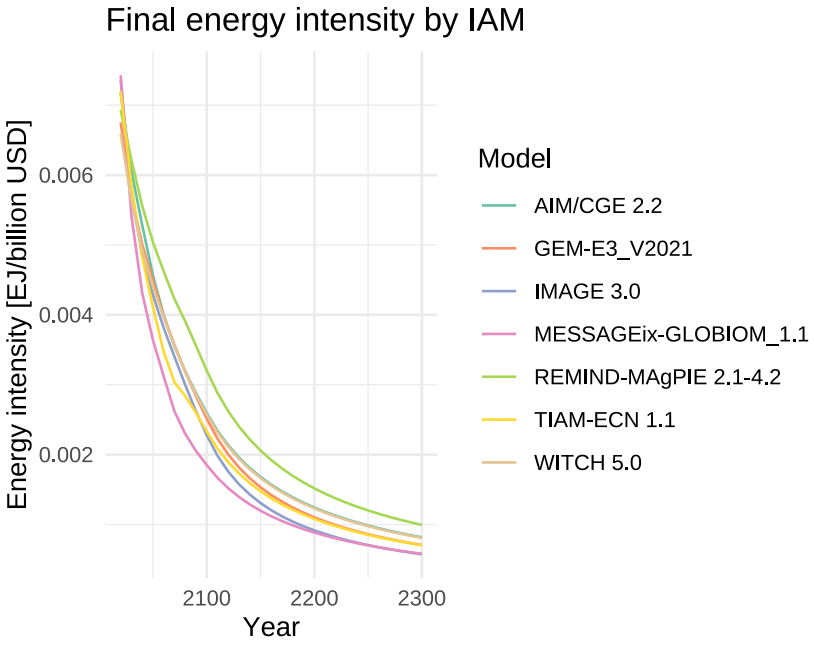

Figure 8: Extrapolated final energy intensity by IAM, in EJ / billion 2010 USD.

For ultra long-term projections beyond 2300, it is assumed that a steady state of net negative emissions will by then be achieved. That is, abatement options will operate at their maximum capacity. To hold net negative emissions at a constant level, baselines are fixed at their 2300 value after this date.

3.2.3 Extrapolation of primary energy

We define a linear phase-out of fossil primary energy $W_{\text{foss}}(t)$, starting from its value at time $t_0 = 2100$, denoted as $W_{\text{foss}}(t_0)$, and decreasing to zero by a specified end year. The phase-out proceeds at a constant rate and is expressed as:

$$W_{\text{foss}}(t) = \max\left(W_{\text{foss}}(t_0) \cdot \left(1 - \frac{t - t_0}{t_{\text{end}} - t_0}\right), 0\right)$$

where $t \geq t_0$. The formulation ensures that fossil energy use declines linearly to zero by the final year and remains zero thereafter.

Nuclear and bioenergy pathways are determined by using the marginal abatement cost functions under a specified carbon price path. As long as the imposed carbon price remains high enough, abatement via these options continues to grow until an upper bound is reached.

NBRs are assumed to fill the remaining energy demand not met by fossil fuels, bioenergy, or nuclear. The NBR contribution is calculated as the residual required to satisfy final energy demand, adjusted for conversion efficiencies:

$$W_{\text{nbr}}(t) = \frac{1}{\eta_{\text{nbr}}}\left[F(t) - \sum_{i \in \{\text{bio,nuc,foss,trad}\}} \eta_i W_i(t)\right]$$

This approach is justified by the vast physical potential of renewable energy sources such as wind and solar, which are not assumed to be capacity-limited in this long-term extrapolation.

The fossil fuel phase-out trajectory, modulated by potential use of fossil CCS, effectively determines the gross emissions path. If fossil energy use is already low by 2100 (in a high-ambition scenario), it is likely that bioenergy and nuclear options have reached their maximum levels, implying that continued increases in energy demand will be met almost entirely by expanding NBR deployment. In this case, NBRs are already substantial in 2100 and continue to grow approximately in line with final energy demand, which itself depends on economic growth. In contrast, if fossil fuel use remains high in 2100 (a lower-ambition scenario), bioenergy and nuclear may still have room to grow post-2100, partially offsetting the reduction in fossil energy. However, NBRs will also have to expand more aggressively to fill the gap, yet starting from a lower level in 2100.

References

Lint Barrage and William Nordhaus. Policies, projections, and the social cost of carbon: Results from the dice-2023 model. *Proceedings of the National Academy of Sciences*, 121(13):e2312030121, 2024. doi: 10.1073/pnas.2312030121. URL https://www.pnas.org/doi/abs/10.1073/pnas.2312030121.

Robert C. Feenstra, Robert Inklaar, and Marcel P. Timmer. The next generation of the penn world table. *American Economic Review*, 105(10):3150–3182, 2015. doi: 10.1257/aer.20130954. URL https://www.rug.nl/ggdc/productivity/pwt/.

IPCC. *Summary for Policymakers. In: Climate Change 2022: Mitigation of Climate Change. Contribution of Working Group III to the Sixth Assessment Report of the Intergovernmental Panel on Climate Change*. Cambridge University Press, Cambridge, UK and New York, NY, USA, 2022. doi: 10.1017/9781009157926.001.

Samir K.C., Mohit Dhakad, Michaela Potančoková, Sushil Adhikari, Dilek Yildiz, Marija Mamolo, Tomáš Sobotka, Krystof Zeman, Guy J. Abel, Wolfgang Lutz, and Anne Goujon. Updating the shared socioeconomic pathways (ssps) global population and human capital projections. IIASA Working Paper WP-24-003, International Institute for Applied Systems Analysis, Laxenburg, Austria, 2024. URL https://pure.iiasa.ac.at/id/eprint/19487/.

Marian Leimbach, Elmar Kriegler, Niklas Roming, and Jana Schwanitz. Future growth patterns of world regions – a gdp scenario approach. *Global Environmental Change*, 42:215–225, 2017. ISSN 0959-3780. doi: https://doi.org/10.1016/j.gloenvcha.2015.02.005. URL https://www.sciencedirect.com/science/article/pii/S0959378015000242.

PIK Potsdam Institute for Climate Impact Research. Remind 2.1.0 documentation: Carbon dioxide removal (cdr). https://rse.pik-potsdam.de/doc/remind/2.1.0/33_CDR.htm#b-dac. Accessed: 2025-06-25.

G. Realmonte, L. Drouet, A. Gambhir, J. Glynn, A. Hawkes, A. C. Köberle, and M. Tavoni. An inter-model assessment of the role of direct air capture in deep mitigation pathways. *Nature Communications*, 10:3277, 2019. doi: 10.1038/s41467-019-10842-5. URL https://doi.org/10.1038/s41467-019-10842-5.

A Additional Figures

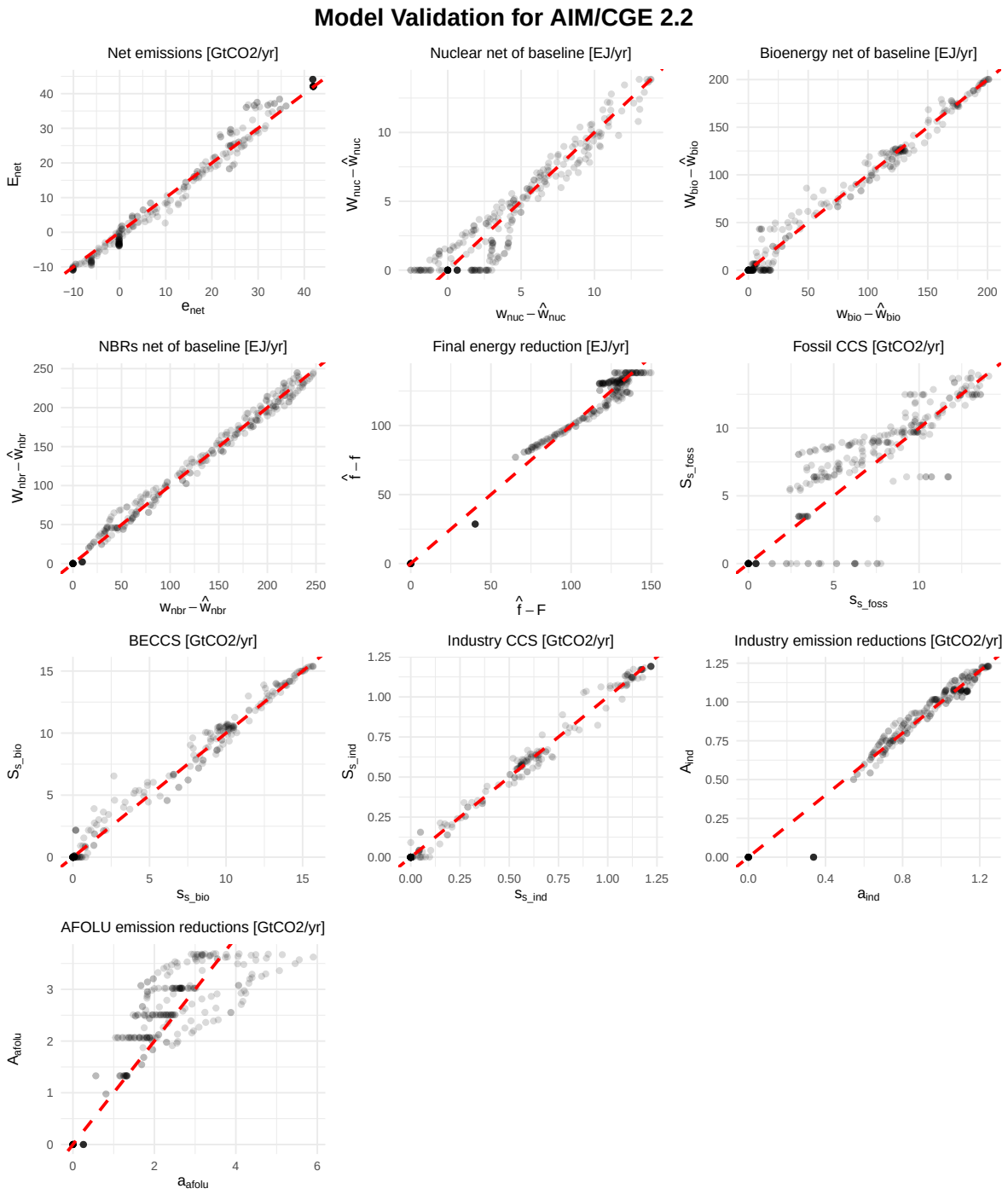

Figure 9: Model Validation for the AIM/CGE 2.2 IAM. Panels displaying emissions and removals (Net Emissions, Fossil CCS, BECCS, DACCS, Industry CCS, Industry Emission Reductions, AFOLU Emission Reductions) are presented in $GtCO_2$/yr, while panels showing energy figures (Nuclear, Bioenergy, NBRs, Final Energy) are in EJ/yr.

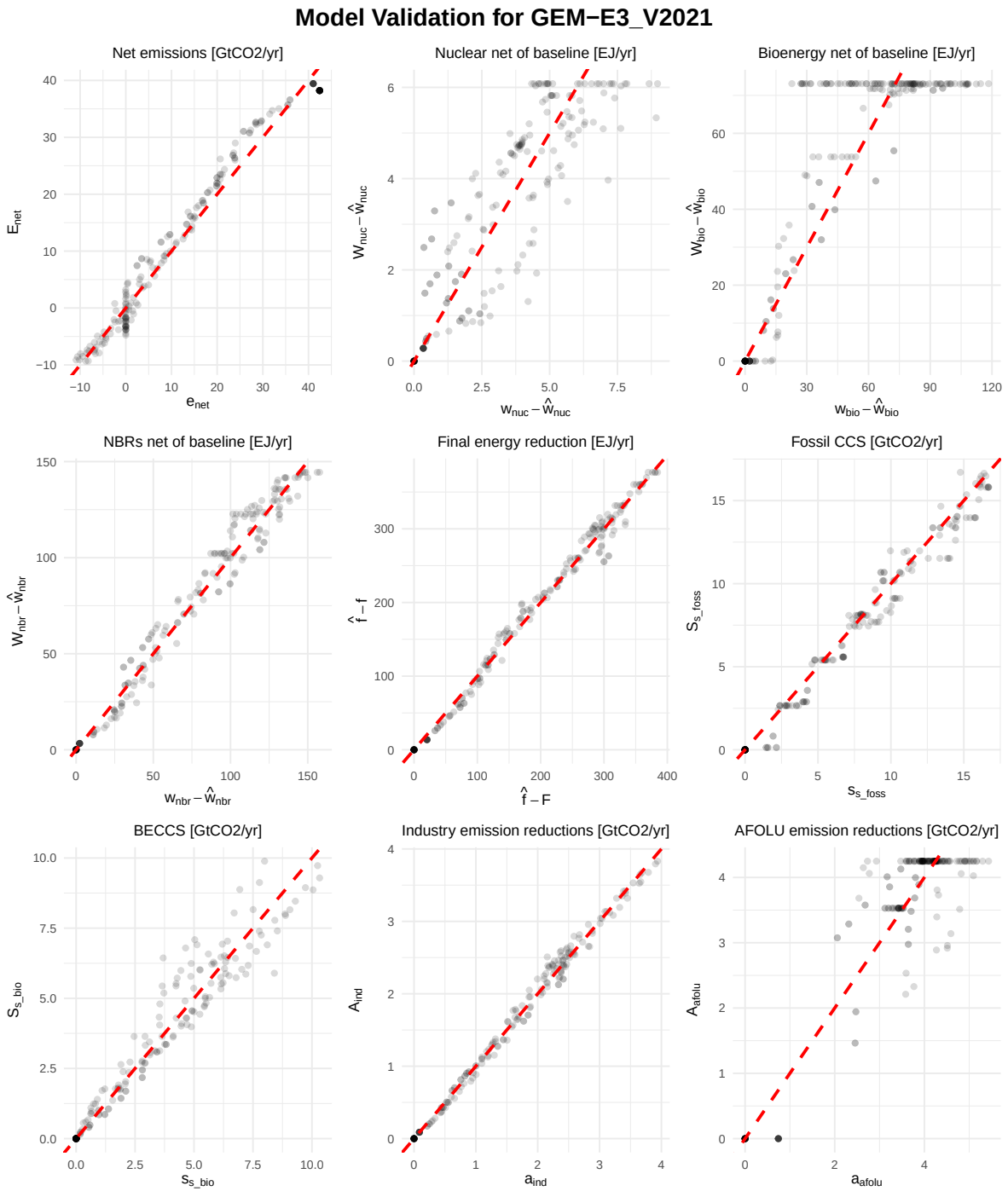

Figure 10: Model Validation for the GEM-E3 IAM. Panels displaying emissions and removals (Net Emissions, Fossil CCS, BECCS, DACCS, Industry CCS, Industry Emission Reductions, AFOLU Emission Reductions) are presented in $GtCO_2$/yr, while panels showing energy figures (Nuclear, Bioenergy, NBRs, Final Energy) are in EJ/yr.

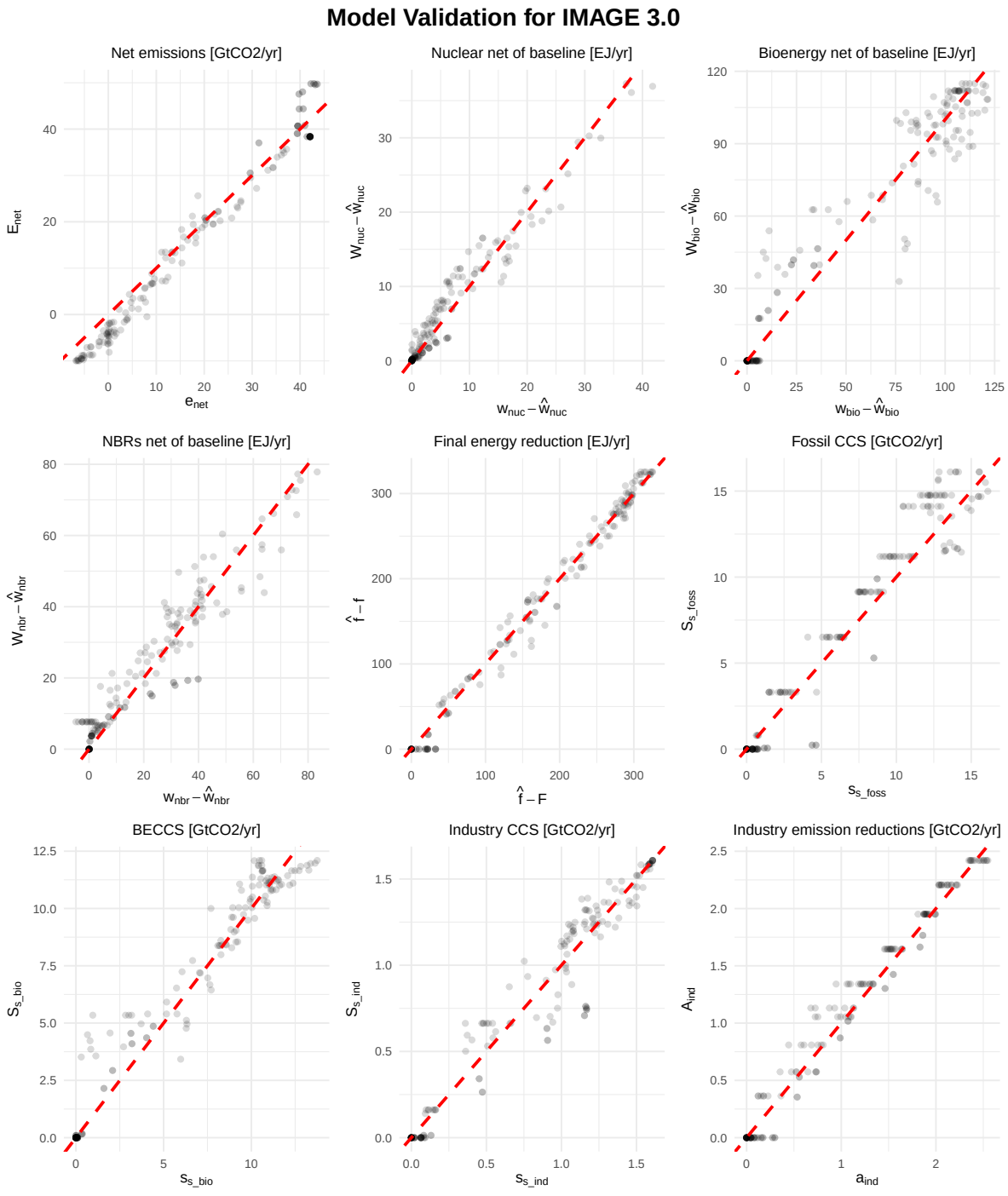

Figure 11: Model Validation for the IMAGE 3.0 IAM. Panels displaying emissions and removals (Net Emissions, Fossil CCS, BECCS, DACCS, Industry CCS, Industry Emission Reductions, AFOLU Emission Reductions) are presented in $GtCO_2$/yr, while panels showing energy figures (Nuclear, Bioenergy, NBRs, Final Energy) are in EJ/yr.

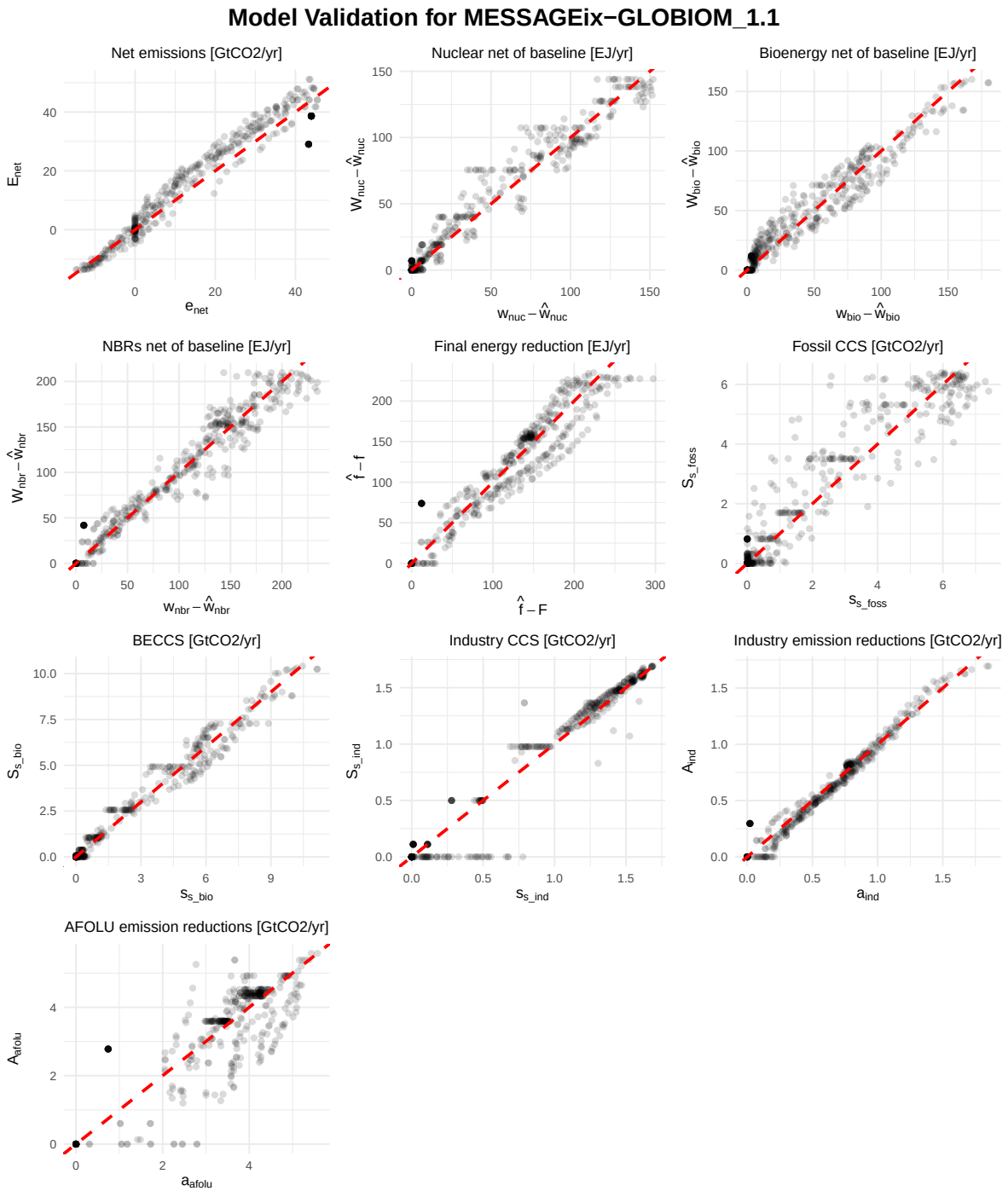

Figure 12: Model Validation for the MESSAGEix-GLOBIOM 1.1 IAM. Panels displaying emissions and removals (Net Emissions, Fossil CCS, BECCS, DACCS, Industry CCS, Industry Emission Reductions, AFOLU Emission Reductions) are presented in $GtCO_2$/yr, while panels showing energy figures (Nuclear, Bioenergy, NBRs, Final Energy) are in EJ/yr.

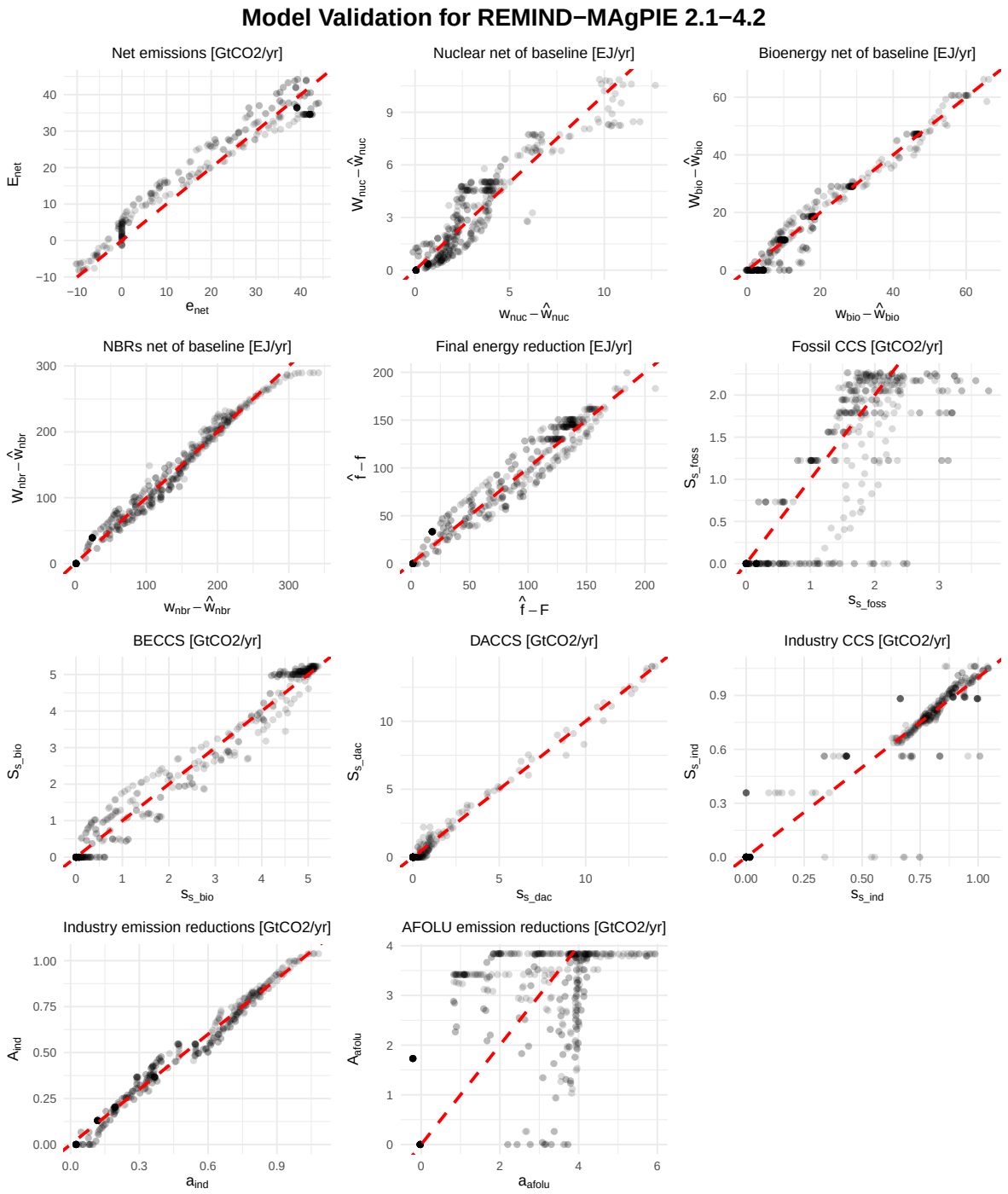

Figure 13: Model Validation for the REMIND-MAgPIE 2.1-4.2 IAM. Panels displaying emissions and removals (Net Emissions, Fossil CCS, BECCS, DACCS, Industry CCS, Industry Emission Reductions, AFOLU Emission Reductions) are presented in $GtCO_2$/yr, while panels showing energy figures (Nuclear, Bioenergy, NBRs, Final Energy) are in EJ/yr.

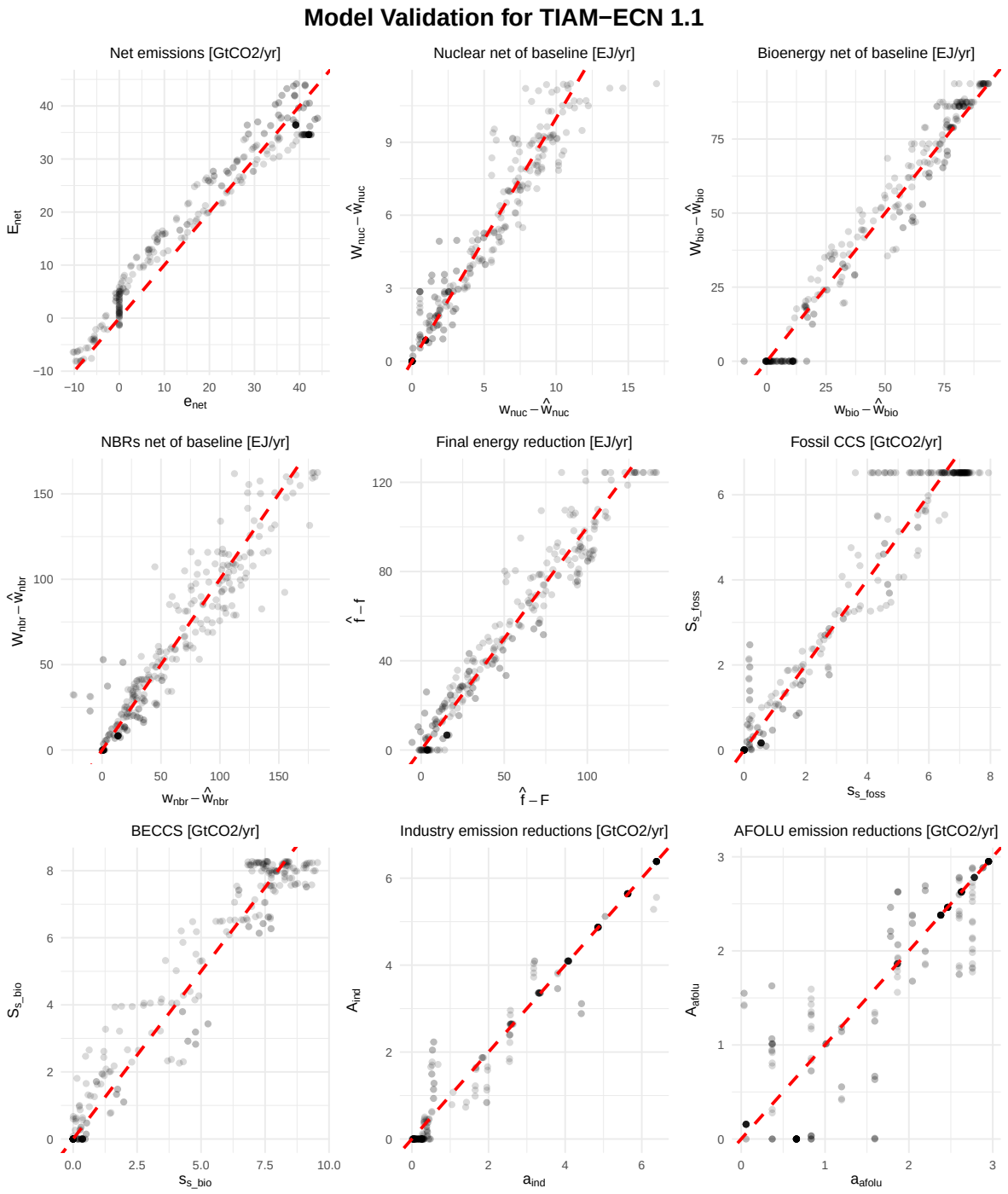

Figure 14: Model Validation for the TIAM-ECN 1.1 IAM. Panels displaying emissions and removals (Net Emissions, Fossil CCS, BECCS, DACCS, Industry CCS, Industry Emission Reductions, AFOLU Emission Reductions) are presented in $GtCO_2$/yr, while panels showing energy figures (Nuclear, Bioenergy, NBRs, Final Energy) are in EJ/yr.

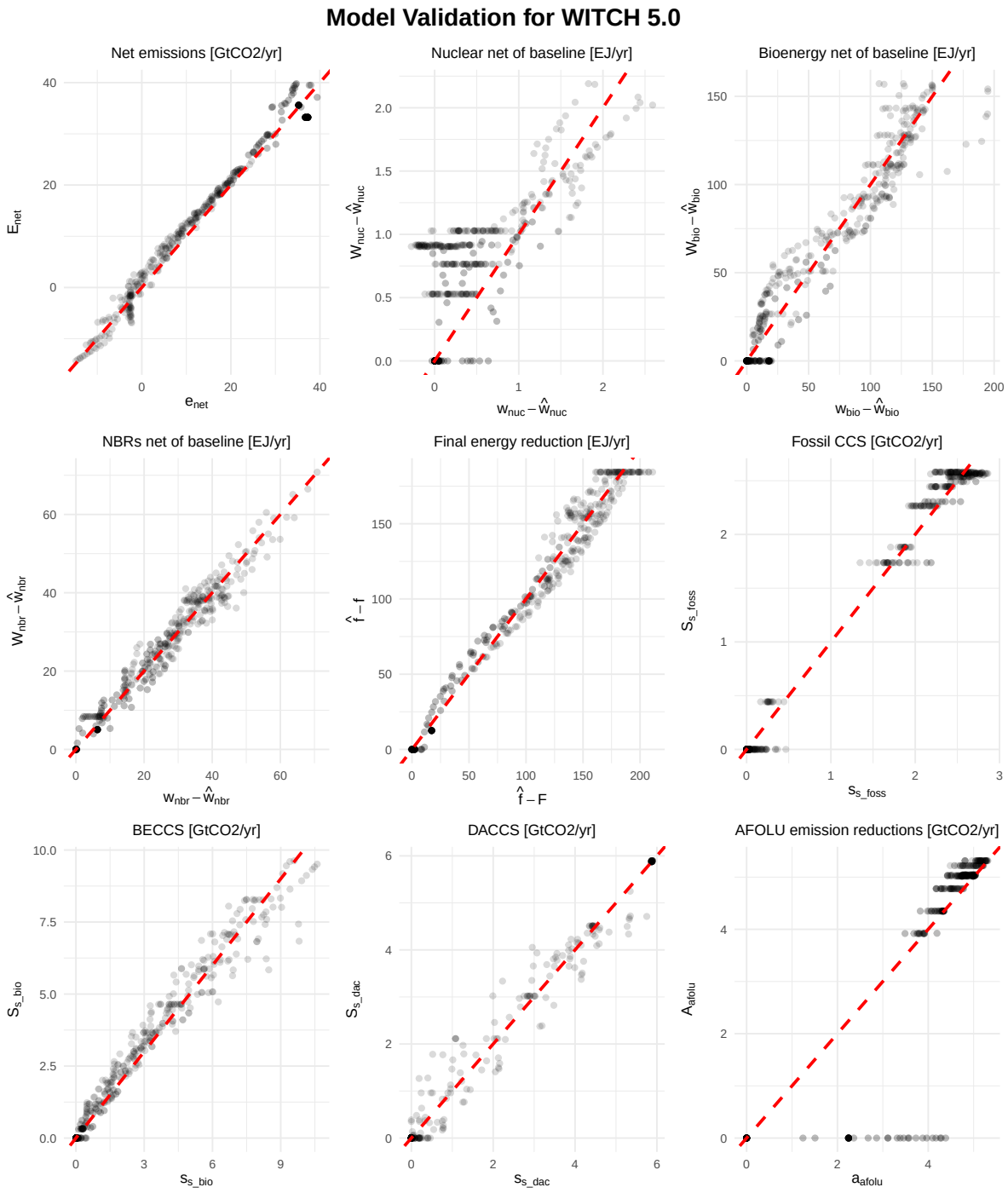

Figure 15: Model Validation for the WITCH 5.0 IAM. Panels displaying emissions and removals (Net Emissions, Fossil CCS, BECCS, DACCS, Industry CCS, Industry Emission Reductions, AFOLU Emission Reductions) are presented in $GtCO_2$/yr, while panels showing energy figures (Nuclear, Bioenergy, NBRs, Final Energy) are in EJ/yr.

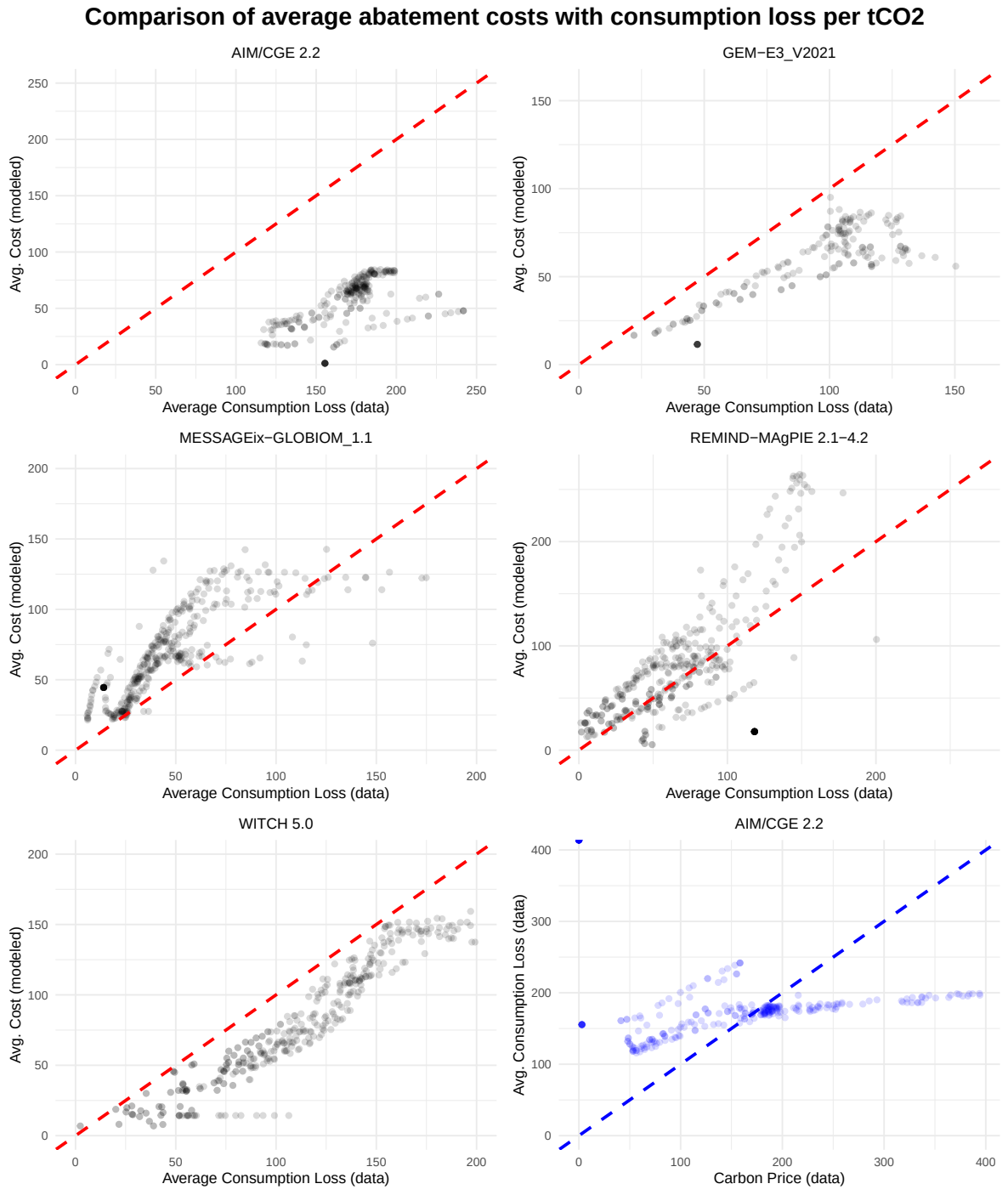

Figure 16: Reported consumption loss per tCO_2 versus modeled total average abatement costs. No consumption loss data are available for IMAGE 3.0 and TIAM-ECN 1.1. For AIM/CGE 2.2, reported consumption loss is also plotted against reported carbon prices (bottom right). If carbon prices represent marginal abatement costs and consumption loss per tCO_2 approximates average costs, then consumption loss should not exceed the carbon price. However, this condition is frequently violated for AIM/CGE 2.2, suggesting that consumption loss may not be a reliable proxy for average abatement costs in this case, which could explain the observed deviation from modeled estimates (top left).

B Model overview

Symbol	Elements	Meaning
$\mathcal{I}$	{foss, nbr, bio, nuc, trad}	Primary energy types: fossil, non-biomass renewables, biomass, nuclear, traditional biomass
$\mathcal{N}$	{ind, afolu}	Sectors: industry, AFOLU (Agriculture, Forestry, and Other Land Use)
$\mathcal{J}$	$\mathcal{N} \cup$ {ener}	Sectors: energy, industry, AFOLU
$\mathcal{K}$	{s_foss, s_bio, s_ind, s_dac}	Carbon capture types: fossil CCS, BECCS, industry CCS, DACCS
$\mathcal{M}$	$\mathcal{I} \cup \mathcal{N} \cup \mathcal{K} \cup$ {fe}	Abatement options: primary energy types, industry, AFOLU, capture types, final energy reduction

Table 7: Index sets used in the model: symbols, elements, and meanings.

Symbol	Explanation	Units
W_i	Primary energy of type $i, i \in \mathcal{I}$	EJ/yr
W_{foss}	Primary energy from fossil fuels	EJ/yr
W_{nbr}	Primary energy from non-biomass renewables	EJ/yr
W_{bio}	Primary energy from biomass	EJ/yr
W_{nuc}	Primary energy from nuclear	EJ/yr
W_{trad}	Primary energy from traditional biomass	EJ/yr
F	Final energy	EJ/yr
E_{net}	Net emissions (all sectors)	$GtCO_2$/yr
E_j	Pre-capture emissions from sector $j, j \in \mathcal{J}$	$GtCO_2$/yr
E_{ener}	Pre-capture emissions from energy system	$GtCO_2$/yr
E_{ind}	Pre-capture industrial process emissions	$GtCO_2$/yr
E_{afolu}	Net emissions from AFOLU	$GtCO_2$/yr
S_k	Carbon captured/stored via option k	$GtCO_2$/yr
$S_{\text{s\_foss}}$	Capture via fossil CCS	$GtCO_2$/yr
$S_{\text{s\_bio}}$	Removals via BECCS	$GtCO_2$/yr
$S_{\text{s\_ind}}$	Capture via industry CCS	$GtCO_2$/yr
$S_{\text{s\_dac}}$	Removals via DACCS	$GtCO_2$/yr
A_{fe}	Abatement from reducing final energy	$GtCO_2$/yr
A_i	Abatement from substituting fossils fuels with primary energy source i	$GtCO_2$/yr
ΔW_i	Change in primary energy i vs baseline, $i \in \mathcal{I}$	EJ/yr
ΔF	Change in final energy vs baseline	EJ/yr
$v_i(t)$	Upper bound on $W_i(t), \quad i \in \mathcal{I} \setminus$ {foss}	EJ/yr
$v_j(t)$	Upper bound on abatement in sector $j, j \in \mathcal{N}$	$GtCO_2$/yr
$v_k(t)$	Upper bound on capture option $k, k \in \mathcal{K}$	$GtCO_2$/yr
$v_k^{\text{pot}}(t)$	Technical capture potential of option $k, k \in \mathcal{K} \setminus$ {s_dac}	$GtCO_2$/yr
$v_{\text{fe}}(t)$	Lower bound on final energy	EJ/yr

Table 8: Model variables with brief explanation and units.

Energy and emission balance:

$$E_{\text{net}}(t) = \sum_{j \in \mathcal{J}} E_j(t) - \sum_{k \in \mathcal{K}} S_k(t); \tag{10}$$

$$E_{\text{ener}}(t) = \beta_{\text{foss}} W_{\text{foss}}(t); \tag{11}$$

$$F(t) = \sum_{i \in \mathcal{I}} \eta_i W_i(t). \tag{12}$$

Symbol	Meaning	Units
$\hat{\cdot}$	hat notation is used to distinguish between elements from the baseline and mitigation scenarios.	
$\hat{W}_i(t)$	Baseline primary energy of type $i, i \in \mathcal{I}$	EJ/yr
$\hat{E}_j(t)$	Baseline pre-capture emissions from sector $j, j \in \mathcal{N}$	$GtCO_2$/yr
$\hat{S}_k(t)$	Baseline carbon captured/stored via option $k, k \in \mathcal{K}$	$GtCO_2$/yr
β_{foss}	Carbon intensity of fossil fuels	$GtCO_2$/EJ
η_i	Conversion efficiency from primary to final energy for type $i, i \in \mathcal{I}$	–
σ_i	Substitution efficiency of fuel i vs fossil fuels, $i \in \mathcal{I} \setminus \{\text{foss}\}$	–
d_i, u_i	Marginal cost floor/ceiling for option $i, i \in \mathcal{I} \setminus \{\text{foss}\}$	USD/tCO_2
l_i	Lag parameter for option $i, i \in \mathcal{I} \setminus \{\text{foss}\}$	–
a_i, b_i	Cost function coefficients for option $i, i \in \mathcal{I} \setminus \{\text{foss}\}$	see cost eq.
g_i	Growth parameter for max abatement change for option $i, i \in \mathcal{I} \setminus \{\text{foss}\}$	$GtCO_2$/yr

Table 9: Model parameters with meanings and units.

Initial conditions and assumptions:

$$W_i(t_0) := \hat{W}_i(t_0), \tag{13}$$
$$F(t_0) := \hat{F}(t_0), \tag{14}$$
$$S_k(t_0) := \hat{S}_k(t_0), \tag{15}$$
$$\Delta W_{\text{trad}}(t) = 0. \tag{16}$$

Abatement:

$$\Delta W_i(t) := \hat{W}_i(t) - W_i(t), \quad i \in \mathcal{I}; \tag{17}$$
$$A(t) := \beta_{\text{foss}} \Delta W_{\text{foss}}(t); \tag{18}$$
$$\sigma_i := \frac{\eta_i}{\eta_{\text{foss}}}, \quad i \in \mathcal{I} \setminus \{\text{foss}\}; \tag{19}$$
$$A_i(t) := -\beta_{\text{foss}} \sigma_i \Delta W_i(t), \quad i \in \mathcal{I} \setminus \{\text{foss}\}; \tag{20}$$
$$\Delta F(t) := \hat{F}(t) - F(t); \tag{21}$$
$$A_{\text{fe}}(t) := \frac{\beta_{\text{foss}} \Delta F(t)}{\eta_{\text{foss}}}; \tag{22}$$
$$A_j(t) := \hat{E}_j(t) - E_j(t), \quad j \in \mathcal{N}; \tag{23}$$
$$A_k(t) := S_k(t) - \hat{S}_k(t), \quad k \in \mathcal{K}. \tag{24}$$

Marginal costs, total costs, and limits for abatement through primary energy substitution:

For $i \in \mathcal{I} \setminus \{\text{foss}\}$

$$P_i(t) = \begin{cases} \frac{a_i}{(\beta_{\text{foss}} \sigma_i)^{b_i}} (A_i(t) - l_i A_i(t-1))^{b_i} + d_i, & \text{if } A_i(t) \geq l_i A_i(t-1) \\ d_i, & \text{if } A_i(t) < l_i A_i(t-1) \end{cases}; \tag{25}$$

$$C_i(t) = \begin{cases} \frac{a_i}{b_i + 1} \left(\frac{1}{(\beta_{\text{foss}} \sigma_i)^{b_i}} (A_i(t) - l_i A_i(t-1))^{b_i+1} \right) + d_i A_i(t), & \text{if } A_i(t) \geq l_i A_i(t-1) \\ d_i A_i(t), & \text{if } A_i(t) < l_i A_i(t-1) \end{cases}; \tag{26}$$

$$W_i(t) \leq v_i(t), \tag{27}$$
$$A_i(t) \leq \beta_{\text{foss}} \sigma_i g_i + l_i A_i(t-1). \tag{28}$$

Marginal costs, total costs, and limits for abatement through final energy reduction:

$$P_{\text{fe}}(t) = \begin{cases} a_{\text{fe}} \left(\frac{\eta_{\text{foss}}}{\beta_{\text{foss}}} \right)^{b_{\text{fe}}} (A_{\text{fe}}(t) - l_{\text{fe}} A_{\text{fe}}(t-1))^{b_{\text{fe}}} + d_{\text{fe}}, & \text{if } A_{\text{fe}}(t) \geq l_{\text{fe}} A_{\text{fe}}(t-1) \\ d_{\text{fe}}, & \text{if } A_{\text{fe}}(t) < l_{\text{fe}} A_{\text{fe}}(t-1) \end{cases}; \tag{29}$$

$$C_{\text{fe}}(t) = \begin{cases} \frac{a_{\text{fe}}}{b_{\text{fe}}+1} \left(\frac{\eta_{\text{foss}}}{\beta_{\text{foss}}} \right)^{b_{\text{fe}}} (A_{\text{fe}}(t) - l_{\text{fe}} A_{\text{fe}}(t-1))^{b_{\text{fe}}+1} + d_{\text{fe}} A_{\text{fe}}(t), & \text{if } A_{\text{fe}}(t) \geq l_{\text{fe}} A_{\text{fe}}(t-1) \\ d_{\text{fe}} A_{\text{fe}}(t), & \text{if } A_{\text{fe}}(t) < l_{\text{fe}} A_{\text{fe}}(t-1) \end{cases}; \tag{30}$$

$$F(t) \geq v_{\text{fe}}(t), \tag{31}$$
$$A_{\text{fe}}(t) \leq \frac{\beta_{\text{foss}}}{\eta_{\text{foss}}} g_{\text{fe}} + l_{\text{fe}} A_{\text{fe}}(t-1). \tag{32}$$

Marginal costs, total costs, and limits for abatement in industry and AFOLU sector:

For $j \in \mathcal{N}$,

$$P_j(t) = \begin{cases} a_j (A_j(t) - l_j A_j(t-1))^{b_j} + d_j, & \text{if } A_j(t) \geq l_j A_j(t-1) \\ d_j, & \text{if } A_j(t) < l_j A_j(t-1) \end{cases}; \tag{33}$$

$$C_j(t) = \begin{cases} \frac{a_j}{b_j+1} (A_j(t) - l_j A_j(t-1))^{b_j+1} + d_j A_j(t), & \text{if } A_j(t) \geq l_j A_j(t-1) \\ d_j A_j(t), & \text{if } A_j(t) < l_j A_j(t-1) \end{cases}; \tag{34}$$

$$A_j(t) \leq v_j(t), \tag{35}$$
$$A_j(t) \leq g_j + l_j A_j(t-1). \tag{36}$$

Marginal costs, total costs, and limits for carbon capture:

For $k \in \mathcal{K}$,

$$P_k(t) = \begin{cases} a_k \left(A_k(t) - l_k A_k(t-1) \right)^{b_k} + d_k, & \text{if } A_k(t) \geq l_k A_k(t-1) \\ d_k A_k(t), & \text{if } A_k(t) < l_k A_k(t-1) \end{cases}; \tag{37}$$

$$C_k(t) = \begin{cases} \frac{a_k}{b_k+1} (A_k(t) - l_k A_k(t-1))^{b_k+1} + d_k A_k(t), & \text{if } A_k(t) \geq l_k A_k(t-1) \\ d_k A_k(t), & \text{if } A_k(t) < l_k A_k(t-1) \end{cases}; \tag{38}$$

$$S_k(t) \leq v_k(t), \tag{39}$$
$$A_k(t) \leq g_k + l_k A_k(t-1). \tag{40}$$

C Abatement functions

C.1 Abatement functions for primary energy substitution

The marginal and total cost functions introduced in Sections 1.5 to 1.7 can be used to solve for abatement under a specified objective function in an optimization framework. In contrast, simulation and calibration require functions that directly determine abatement from an exogenous carbon price path $P(\cdot)$. Here, we introduce such abatement functions. In essence, we show how a given global carbon price path $P(\cdot)$ generates a feasible trajectory for $W_i(\cdot)$, and thus for $A_i(\cdot)$, with the corresponding marginal costs $P_i(\cdot)$ computed as described in Section C.1.1.

For computing pathways of primary energy sources, we define the following function:

$$W_i(t) = \min\left(\widetilde{a}_i \widetilde{P}_i(t)^{\widetilde{b}_i} - l_i \Delta W_i(t-1) + \hat{W}_i(t),\ v_i(t)\right), \tag{41}$$

with

$$\widetilde{P}_i(t) := \min(u_i, P(t)) - \min(d_i, P(t)),$$

where $u_i \geq d_i$. The parameters d_i and u_i denote the marginal cost floor and ceiling, below and above which the imposed carbon price has no effect on abatement. The parameter $v_i(t)$ specifies the maximum achievable value of $W_i(t)$ in each period. Recall that $\Delta W_i(t) = -\frac{A_i(t)}{\beta_{\text{foss}}\sigma_i}$ (see Eq. 3). Moreover, we define the transformations $\widetilde{a}_i := a_i^{-1/b_i}$, $\widetilde{b}_i := 1/b_i$, and $g_i := \widetilde{a}_i(u_i - d_i)^{\widetilde{b}_i}$.

Case A
Suppose

$$\widetilde{a}_i \widetilde{P}_i(t)^{\widetilde{b}_i} - l_i \Delta W_i(t-1) + \hat{W}_i(t) \leq v_i(t).$$

Then,

$$W_i(t) = \widetilde{a}_i \widetilde{P}_i(t)^{\widetilde{b}_i} - l_i \Delta W_i(t-1) + \hat{W}_i(t).$$

Let us now analyze $\widetilde{P}_i(t)$.
Case A.1 – Standard case ($d_i < P(t) < u_i$), hence, $\widetilde{P}_i(t) = P(t) - d_i$. Substituting yields:

$$W_i(t) - \hat{W}_i(t) + l_i \Delta W_i(t-1) = \widetilde{a}_i \big(P(t) - d_i\big)^{\widetilde{b}_i}.$$

Hence,

$$\big(\widetilde{a}_i^{-1}(W_i(t) - \hat{W}_i(t) + l_i \Delta W_i(t-1))\big)^{1/\widetilde{b}_i} = P(t) - d_i,$$

and therefore,

$$P(t) = a_i \big(W_i(t) - \hat{W}_i(t) + l_i \Delta W_i(t-1)\big)^{b_i} + d_i.$$

Substituting $A_i(t) = -\beta_{\text{foss}}\sigma_i \Delta W_i(t)$ yields:

$$P(t) = \frac{a_i}{(\beta_{\text{foss}}\sigma_i)^{b_i}} \big(A_i(t) - l_i A_i(t-1)\big)^{b_i} + d_i, \tag{42}$$

Thus, in this carbon price range, $P_i(t) := P(t)$.

Case A.2 – Price ceiling ($P(t) > u_i$) Here, $\widetilde{P}_i(t) = u_i - d_i$. Inserting into Eq. 41 gives

$$A_i(t) = \beta_{\text{foss}}\sigma_i g_i + l_i A_i(t-1),$$

which represents the maximum feasible per-period growth (compare with Eq. 6). To determine the marginal costs at the maximum growth, we substitute this expression into Eq. 4 and obtain $P_i(t) = u_i$.

Case A.3 – Price floor ($P(t) < d_i$) Here, $\widetilde{P}_i(t) = 0$. Then, again inserting into Eq. 41 gives

$$A_i(t) = l_i A_i(t-1).$$

This is a lower bound for abatement growth by period. Inserting this into Eq. 4 yields the marginal cost at the lowest possible growth, $P_i(t) = d_i$.

Summary Case A Given the condition

$$\widetilde{a}_i \widetilde{P}_i(t)^{\widetilde{b}_i} - l_i \Delta W_i(t-1) + \hat{W}_i(t) \leq v_i(t),$$

we have shown:

- The lowest feasible abatement growth is given by $A_i(t) = l_i A_i(t-1)$.
- The largest feasible abatement growth is given by $A_i(t) = \beta_{\text{foss}}\sigma_i g_i + l_i A_i(t-1)$.
- Marginal costs satisfy:

$$P_i(t) = \frac{a_i}{(\beta_{\text{foss}}\sigma_i)^{b_i}} \big(A_i(t) - l_i A_i(t-1)\big)^{b_i} + d_i.$$

So far, we have only considered the upper part of the marginal cost function in Eq 4.

Case B

Suppose

$$\widetilde{a}_i \widetilde{P}_i(t)^{\widetilde{b}_i} - l_i \Delta W_i(t-1) + \hat{W}_i(t) > v_i(t).$$

Then,

$$W_i(t) = v_i(t),$$

which reflects Eq. 5, and from which $A_i(t)$ can be inferred:

$$A_i(t) = \beta_{\text{foss}}\sigma_i(v_i(t) - \hat{W}_i(t)). \tag{43}$$

C.1.1 Link between carbon price an marginal costs

For **Case A**, we have established a relation between the price path $P(t)$ and abatement-option-specific marginal costs $P_i(t)$:

$$P_i(t) = \begin{cases} P(t), & d_i \leq P(t) \leq u_i, \\ d_i, & P(t) < d_i, \\ u_i, & P(t) > u_i, \end{cases}$$

where $P(t)$ is the globally imposed carbon price, while $P_i(t)$ denotes the abatement-option-specific marginal cost. For **Case B**, abatement is trivially derived from Eq. 43, which can be used in Eq. 4 to determine $P_i(t)$. In **Case B** $P_i(t)$ in any case diverges from $P(t)$. Finally note that, **Case A** is limited to solutions $l_i A_i(t-1) \leq A_i(t) \leq \beta_{\text{foss}} \sigma_i g_i + l_i A_i(t-1)$. **Case B** can lead to solutions where $A_i(t) < l_i A_i(t-1)$, for which $P_i(t) = d_i$. Moreover, if we have $P(t) < d_i$ and $\widetilde{a}_i \widetilde{P}_i(t)^{\widetilde{b}_i} - l_i \Delta W_i(t-1) + \hat{W}_i(t) > v_i(t)$, it follows that $A_i(t) < l_i A_i(t-1)$.

C.2 Abatement function for final energy reduction

The abatement function for final energy reduction differs from those for primary energy substitution in terms of the signs. We have the following form:

$$F(t) = -\min\left(\widetilde{a}_{\text{fe}} \widetilde{P}_{\text{fe}}(t)^{\widetilde{b}_{\text{fe}}} + l_{\text{fe}} \Delta F(t-1) - \hat{F}(t), v_{\text{fe}}(t)\right). \tag{44}$$

Here, $\widetilde{a}_{\text{fe}} \leq 0$ and $v_{\text{fe}}(t)$ is the minimum allowable amount of $F_i(t)$. Using the definitions $a_{\text{fe}} := |\widetilde{a}_{\text{fe}}|^{-1/\widetilde{b}_{\text{fe}}}$, $b_{\text{fe}} := 1/\widetilde{b}_{\text{fe}}$, $g_{\text{fe}} := \left(\frac{u_{\text{fe}} - d_{\text{fe}}}{a_{\text{fe}}}\right)^{1/b_{\text{fe}}}$, and $\Delta F(t) = \frac{\eta_{\text{foss}}}{\beta_{\text{foss}}} A_{\text{fe}}(t)$, we can link Eq. 44 to the marginal cost function 7, following the steps of Section C.1.

C.3 Abatement functions for industry and AFOLU sectors

The abatement functions for Industry and AFOLU sectors are defined as:

$$A_j(t) = \min\left(\widetilde{a}_j \widetilde{P}_j(t)^{\widetilde{b}_j} + l_j A_j(t-1), v_j(t)\right),$$

where $\widetilde{P}_j(t) := \min(u_j, P(t)) - \min(d_j, P(t))$ and $u_j \geq d_j$. As before, using the definitions $\widetilde{a}_j := a_j^{-1/b_j}$, $\widetilde{b}_j := 1/b_j$, and $g_j := \widetilde{a}_j (u_j - d_j)^{\widetilde{b}_j}$, we can link this abatement function, to the marginal cost function in Eq 8 and its associated constraints.

C.4 Abatement functions for carbon capture

The abatement function for carbon capture is defined as:

$$S_k(t) = \min\left(\widetilde{a}_k \widetilde{P}_k(t)^{\widetilde{b}_k} + l_k A_k(t-1) + \hat{S}_k(t), v_k(t)\right),$$

where $\widetilde{P}_k(t) := \min(u_k, P(t)) - \min(d_k, P(t))$ and $u_k \geq d_k$. As before, using $\widetilde{a}_k := a_k^{-1/b_k}$, $\widetilde{b}_k := 1/b_k$, $\delta_k := d_k$, and $g_k := \widetilde{a}_k (u_k - d_k)^{\widetilde{b}_k}$, we can link the abatement function to Eq. 9 and its associated constraints.